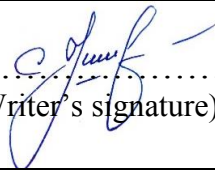




Universitetet
i Stavanger

Faculty of Science and Technology

MASTER'S THESIS

Study program/ Specialization: Offshore Technology / Subsea and Marine Technology	Spring semester, 2018 <u>Open</u> / Restricted access
Writer: Ivan Kurchatov	 (Writer's signature)
Faculty supervisor: Ove Tobias Gudmestad	
External supervisor: Anatoly Borisovich Zolotukhin	
Thesis title: Comparative analysis of the possible development concepts of the North Wrangel license area based on Arctic best available technologies	
Credits (ECTS): 30	
Key words: the Arctic; the North Wrangel license area; the East Siberian Sea; Status of Technology; limiting factors; comparative analysis; weight coefficient; aggregated parameter; feasibility study; iceberg; impact forces; stochastic analysis, gravity based structure; CAPEX.	Pages: _____ 94 +Appendix: _____ 9 Stavanger, _____ 15/06/2018 date / month / year

Abstract

Problem statement and objective

Russia has one of the world's highest mineral and raw materials potential. Current status of the oil and gas recoverable resources in Russia allows maintaining the current level of production. However, according to the Energy Strategy of Russia for the period up to 2035, the exploration and development of hydrocarbon resources in the seas of the Arctic Ocean will be of the highest priority due to unavoidable production decline.

Currently, there is no comprehensive data about the Arctic, so this fact imposes certain restrictions on field development planning and conceptual studies. In particular, this is due to lack of infrastructure in the region as a whole, and especially in the areas that are not enough industrially explored such as the East Siberian Sea, which makes it hard to collect sufficient data for detailed analysis.

The objective of the master's thesis is to develop the basis, which will enable the industry professionals to narrow further detailed conceptual analysis that can be performed as soon as enough data is available. This basis was created by:

- determining the status of technology for extreme Arctic and ranking various best practices applicable for the East Siberian Sea;
- analyzing existing data on environmental conditions;
- calculating possible environmental impacts on the structures;
- identifying limiting factors and challenges;
- developing a new approach to conceptual analysis held in lack-of-data conditions and based on a comparative analysis of environmental conditions of similar regions;

Scope of work

Starting with review of currently acknowledged challenges in the Arctic region, the project comprehensively analyzes environmental conditions of the East Siberian Sea (the North Wrangel license area) and identifies key limiting factors associated with its development. Following, environmental loads on a structure are estimated in order to demonstrate the loads of what range could the structure experience being installed in the area. As a result of this assessment, status of technology for extreme Arctic conditions is considered in order to verify applicability of existing technical and technological solutions for the operations in the license area. Being one of the core aspects of the thesis, possible development concepts study is performed using the analytical mechanism of the aggregated parameters. CAPEX estimates are also provided in the project.

Acknowledgements

First and foremost, I would like to sincerely thank my faculty supervisor Professor Ove Tobias Gudmestad for his continuous help and patience. His expertise and great support have made an outstanding contribution to this work.

I would like to express my deep appreciation to my scientific supervisor from Gubkin University, Professor Anatoly Borisovich Zolotukhin, whose knowledge, experience and valuable ideas inspired and helped me a lot throughout the whole study at the joint master program.

I also would like to thank Professor Sveinung Løset and Aleksey Shestov for their support and foundational knowledge on ice loads evaluation they provided during the course at UNIS.

Special thanks to Dmitry Chernov, specialist at Gazprom Neft Shelf LLC, for his kind help and guiding comments on my master's thesis.

List of contents:

List of figures.....	6
List of tables.....	7
List of abbreviations.....	9
Introduction.....	10
1. Challenges associated with the Arctic.....	11
2. The North-Wrangel license area analysis.....	12
2.1. The license area geographical location.....	12
2.2. Environmental conditions of the license area.....	13
2.2.1. Climate.....	13
2.2.2. Hydrologic characteristics.....	14
2.2.3. Wave conditions.....	16
2.2.4. Ice conditions.....	16
2.2.4.1. Physical and mechanical properties of the ice.....	18
2.2.4.2. Ice drift.....	19
2.2.4.3. Ice-free period.....	20
2.2.4.4. Icebergs.....	20
2.3. Reserves primary evaluation.....	22
2.4. Infrastructure.....	23
2.5. Limiting factors analysis.....	23
3. Estimation of environmental loads on the structure.....	25
3.1. Wave loads.....	25
3.1.1. Theoretical basis for wave loads calculation.....	27
3.1.2. Calculation of wave load on the offshore structures.....	29
3.2. Ice loads.....	30
3.2.1. Theoretical basis for ice loads calculation.....	31
3.2.2. Estimation of ice loads on vertical and sloping structures.....	33
3.2.3. Calculation of iceberg load on cylinder structure.....	36
4. Status of Technology.....	39
4.1. Pechora Sea and Sea of Okhotsk.....	40
4.1.1. “Prirazlomnoye” Project.....	40
4.1.2. Sakhalin Projects (on the example of Arkutun-Dagi field).....	42
4.2. Newfoundland and Labrador Continental Shelf.....	45
4.2.1. “Hibernia” Project.....	46
4.2.2. “Hebron” Project.....	47
4.2.3. “White Rose” Project.....	48
4.3. Cook Inlet and the Beaufort Sea.....	50

4.3.1. Offshore field development in Cook Inlet.....	50
4.3.2. “Molikpaq” Platform.....	53
4.4. Intermediate results and recommendations for further studies.....	56
5. Possible development concepts study.....	58
5.1. Development and ranking criteria for comparison of the regions.....	58
5.2. Comparative analysis of the regions	66
5.3. Selection of the most feasible solution.....	72
5.4. Description of the most feasible field development concepts.....	75
5.4.1. Recommendations on the main structures and facilities for the field development of the North Wrangel license area.....	78
5.4.2. Recommendations on oil transportation.....	81
6. CAPEX estimate for construction of the GBS.....	84
Discussions and conclusion.....	87
List of references.....	88
Appendix A.....	95
Appendix B.....	101

List of figures

Figure 1: License areas of PJSC Gazprom Neft.....	12
Figure 2: Geographical location of the North Wrangel license area.....	13
Figure 3: Annual variation of air temperature.....	13
Figure 4: Distribution of salinity at the surface and at a depth of 40 m in the seas of the eastern sector of the Russian Arctic during the winter and summer period.....	15
Figure 5: Isochrone lines of stable ice formation.....	16
Figure 6: De Long Islands.....	20
Figure 7: Annual probability of occurrence of icebergs.....	21
Figure 8: Glacier cap of Bennett Island.....	21
Figure 9: Iceberg in the East Siberian Sea.....	22
Figure 10: Wave height probability distribution for the East Siberian Sea....	26
Figure 11: Different wave force regimes.....	26
Figure 12: The relation between C_M and D/L	28
Figure 13: Wave profile.....	29
Figure 14: Inertia force distribution along the structure (d=85 m).....	30
Figure 15: Acceleration vs. depth (d=85 m).....	30
Figure 16: Ice impact on the vertical structure.....	34
Figure 17: Ice impact on the sloping structure (rubble accumulation).....	35
Figure 18: IRGBS “Prirazlomnaya”.....	41
Figure 19: Offshore platform “Berkut”.....	44
Figure 20: Offshore platform “Hibernia”.....	46
Figure 21: Hebron platform being towed-out to the field.....	48
Figure 22: Field development concept of the White Rose field.....	49
Figure 23: Offshore platforms of three possible configurations in Cook Inlet	53
Figure 24: Exploratory drilling rig “Molikpaq” in the Beaufort Sea.....	55
Figure 25: Aggregation (grouping) of the environmental parameters.....	60
Figure 26: Dependence on distance to shore.....	77
Figure 27: Schematic representation of possible configurations of the production platform.....	78
Figure 28: Schematic representation of the intermediate platform possible configuration.....	80
Figure 29: Subsea equipment and pipeline burial in the sea bottom.....	81
Figure 30: Concept of oil transportation by the Eastern route.....	82
Figure 31: Direct oil offloading on the example of IRGBS Prirazlomnaya....	82

List of tables

Table 1: 1/100 yr sea disturbance parameters.....	16
Table 2: Ice conditions in the East-Siberian Sea during a year.....	17
Table 3: The average distribution of ice of different ages at the end of ice growth period.....	17
Table 4: Generalization of the ice conditions in the East Siberian Sea.....	18
Table 5: The mechanical characteristics of the sea ice.....	18
Table 6: Ice drift.....	19
Table 7: Input data for wave load calculation.....	25
Table 8: Force regime determination.....	27
Table 9: The results of inertia force calculation.....	29
Table 10: Input data for estimation of ice loads on the vertical structure.....	34
Table 11: The simulation results of ice loads on the vertical structure.....	34
Table 12: Input data for estimation of ice loads on the sloping structure.....	35
Table 13: The simulation results of ice loads on the sloping structure.....	36
Table 14: Input data for estimation of ice loads on the sloping structure.....	37
Table 15: The simulation results of iceberg load.....	38
Table 16: The overall results of ice loads estimation.....	38
Table 17: General information for the North Wrangel license area.....	39
Table 18: General information for the Pechora Sea.....	40
Table 19: General information for the Southern Sea of Okhotsk – off Northeastern Sakhalin-Island Coast.....	43
Table 20: General information for the Newfoundland offshore.....	45
Table 21: The platform key metrics.....	48
Table 22: General information for the Cook Inlet.....	51
Table 23: General information for the Beaufort Sea.....	54
Table 24: Cumulative information on environmental conditions in the considered regions.....	57
Table 25: Description of the comparison criteria ranks.....	62
Table 26: Description of the aggregated comparison criteria ranks.....	63
Table 27: The Rosenberg scale.....	64
Table 28: The results of expert evaluation of the climatic parameters' weight coefficients, using the Rosenberg scale.....	64
Table 29: The results of expert evaluation of the hydrological parameters' weight coefficients, using the Rosenberg scale.....	65
Table 30: The results of expert evaluation of the ice parameters' weight coefficients, using the Rosenberg scale.....	66

Table 31: Ranking the criteria for comparing regions.....	67
Table 32: Ranking the member parameters.....	68
Table 33: Ranking aggregated comparison criteria taking into account weights of member parameters.....	69
Table 34: The results of expert evaluation of the ice parameters' weight coefficients taking into account the lack of data.....	70
Table 35: Comparative analysis of environmental conditions of the license area and the regions.....	70
Table 36: The facilities used for the field development in the analyzed regions.....	72
Table 37: Matrix of the conceptual solutions for the field development in the North Wrangel license area.....	74
Table 38: Parameters of the selected platforms.....	85
Table 39: CAPEX for the construction of various platforms, mln. USD.....	85

List of abbreviations

AARI	– Arctic and Antarctic Research Institute
BTOE	– Billion Tons of Oil Equivalent
CAPEX	– Capital Expenditure
CDC	– Central Drill Center
CIS	– Canadian Ice Service
C-NLOPB	– Canada - Newfoundland & Labrador Offshore Petroleum Board
DNV	– Det Norske Veritas
EOI	– Expression of Interest
FDD	– Freezing Degree Days
FEED	– Front-End Engineering Design
FPSO	– Floating Production Storage Offloading
IRGBS	– Ice-Resistant Gravity Base Structure
IRST	– Ice-Resistant Shuttle Tanker
ISO	– International Organization for Standardization
GBS	– Gravity Based Structure
LLC	– Limited Liability Company
MAC	– Mobile Arctic Caisson
NDC	– Northern Drill Centre
NWLA	– North Wrangel License Area
OLS	– Offshore Loading System
PJSC	– Public Joint Stock Company
POB	– Persons On Board
ppt	– Parts per thousand
SDC	– Southern Drill Center
SPNA	– Special Protected Natural Area
SPS	– Subsea Production System
TCF	– Trillion Cubic Feet

Introduction

Currently, the Russian Federation is investing significant amounts of financial resources in the Arctic. There are several reasons for this. First of all, it should be noted that environmental conditions of the country's main part can be characterized as Arctic or near-Arctic conditions, e.g. almost 70% of the territory is covered with permafrost and approximately 30% is in the Arctic. This can be most clearly described by the words of Admiral Stepan O. Makarov, who said that "Russia is a building which facade is facing the Arctic". Moreover, the Russian part of the Arctic is the richest in petroleum resources. According to the estimates of the Ministry of Natural Resources and Environment, arctic shelves contain ca. 15.5 billion tons of oil and 84.5 TCM gas (~ 100 BTOE = 720 Bbbloe). The forecast of production potential of the Arctic Seas made on the basis of UCube software (Rystad Energy) indicates a sharp increase in hydrocarbons recovery in the region. At the same time, the biggest "jump" is expected in Russia, where the potential is to be increased for several times in comparable with current status in the following decade.

Discoveries of significant reserves of hydrocarbons located in the Arctic shelf require the use of advanced technical solutions for field development. This is also an incentive for the development of new concepts of offshore structures, platforms and equipment designed to operate in harsh climatic conditions.

1. Challenges associated with the Arctic

Industrial interest in the continental shelf of the Arctic has increased significantly over the past decades, especially after the discovery of significant hydrocarbon reserves. However, along with the colossal resource base and related opportunities, there are obvious challenges, among which the most significant are:

- Environmental risks;
- Harsh climate conditions;
- Presence of multiyear ice;
- Need for large capital investments;
- Significant remoteness from the main markets;
- Insufficient level of technologies and competencies development;
- Lack of qualified personnel;
- Emergency response time (*Zolotukhin, 2016*).

Replacement of the resource base is an important component of sustainable development of the extractive industries. This is usually provided by large-scale projects in new petroleum provinces, e.g. Eastern Siberia, Russian Far East and Arctic offshore. For instance, the experts consider Eastern Siberia to have the highest reserve replacement factor, although the amount of necessary capital investments there is almost twice as large as in traditional production regions (*Zolotukhin, 2011*). Arctic continental shelf in this respect is even more challenging due to insufficiency of the technological development and lack of competencies. These are considered as additional factors complicating development of the fields, most of which are located thousands of kilometers from major export hubs and regional centers.

Another challenge is development facilities, which shall be designed in such a way to provide resistance to external loads exerted by sea ice, currents, waves (during ice-free season), etc. In addition, some regions like the Sea of Okhotsk are characterized by high seismic activity, which in turn imposes additional requirements for design and construction of the bottom-fixed facilities. Such modifications significantly increase costs and require large investments in R&D.

Arctic offshore field development is impossible without taking special measures adapted to extreme climatic conditions, to ensure safety and environmental protection. Taking into account the risks associated with decontamination of possible oil spills in ice conditions, the greatest concern is the impact this may have on the fragile Arctic ecosystem (*Zolotukhin, 2011*). This is a matter of responsible business operations by the players owning asset portfolios in the Arctic region.

2. The North-Wrangel license area analysis

The East Siberian Sea is a marginal sea of the Arctic Ocean, located between the Novosibirsk Islands and Wrangel Island. The surface area is 944,600 km². In the west, the East Siberian Sea borders on the Laptev Sea. In the east, it borders on the Chukchi Sea. The northern boundary of the East Siberian Sea passes through an isobath of 200 m. The coast adjacent to the western part of the sea (from Novosibirsk Islands to Kolyma River) is a low-land area. In the eastern part (from Kolyma River to Long Strait), the coast is mountainous, sometimes precipitous. The shoreline is relatively indistinct but forms bays: Chaun Bay, Kolyma Bay, Omulyakhskaya Gulf and Khromskaya Gulf. Large rivers flow into the East Siberian Sea: Kolyma, Alazeya, Indigirka, Khroma (*Prokhorov, 1974*).

The North-Wrangel license area is located in the eastern part of the East Siberian Sea and in the western part of the Chukchi Sea. The right to geological study, exploration and production was obtained by PJSC Gazprom Neft in June 2014. The operator of the project is the company's subsidiary Gazprom Neft Sakhalin LLC (*Gazprom Neft PJSC webpage, n.d.*).

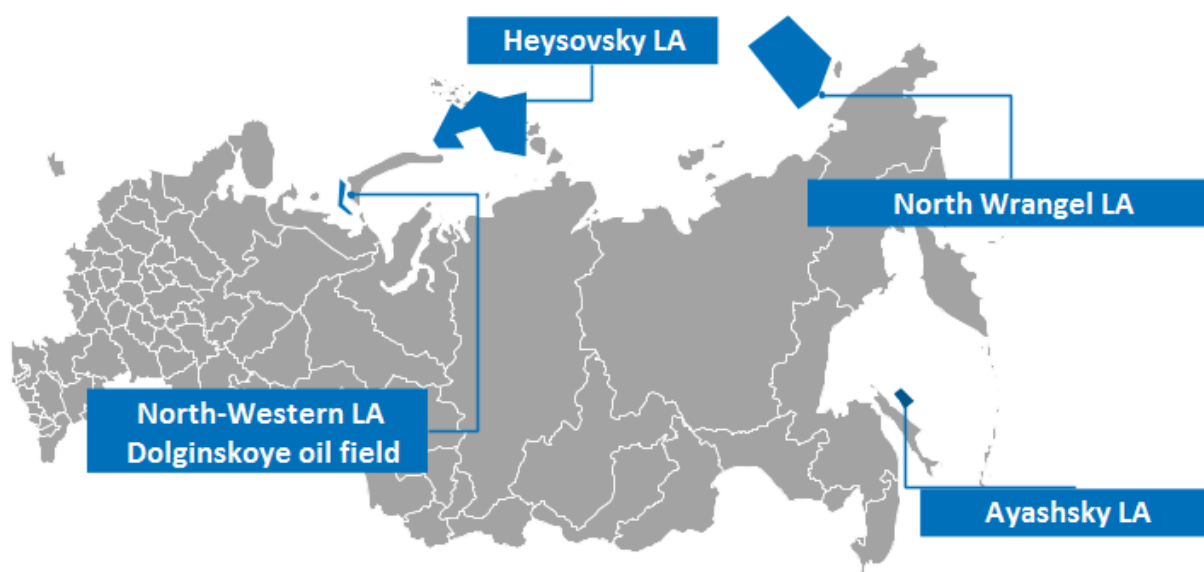


Figure 1: License areas of PJSC Gazprom Neft (*Gazprom Neft Sakhalin webpage, n.d.*)

2.1. The license area geographical location

The North-Wrangel license area is located in the immediate vicinity of the Wrangel and Herald Islands (Figure 2). Wrangel Island is a specially protected natural area of the federal level and an object protected by UNESCO.

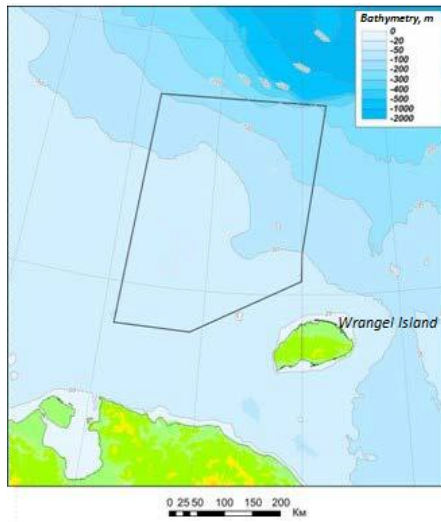


Figure 2: Geographical location of the North-Wrangel license area (Macnab et al., 2002)

2.2. Environmental conditions of the license area

2.2.1. Climate

According to Arctic and Antarctic Research Institute (St. Petersburg, Russia) meteorological data, minimum winter temperatures in the area normally reach -45°C and maximum summer temperatures can range from $+16^{\circ}\text{C}$ to $+18^{\circ}\text{C}$.

The annual variation of monthly average, maximum and minimum air temperatures at the North-Wrangel license area is shown in the graph below.

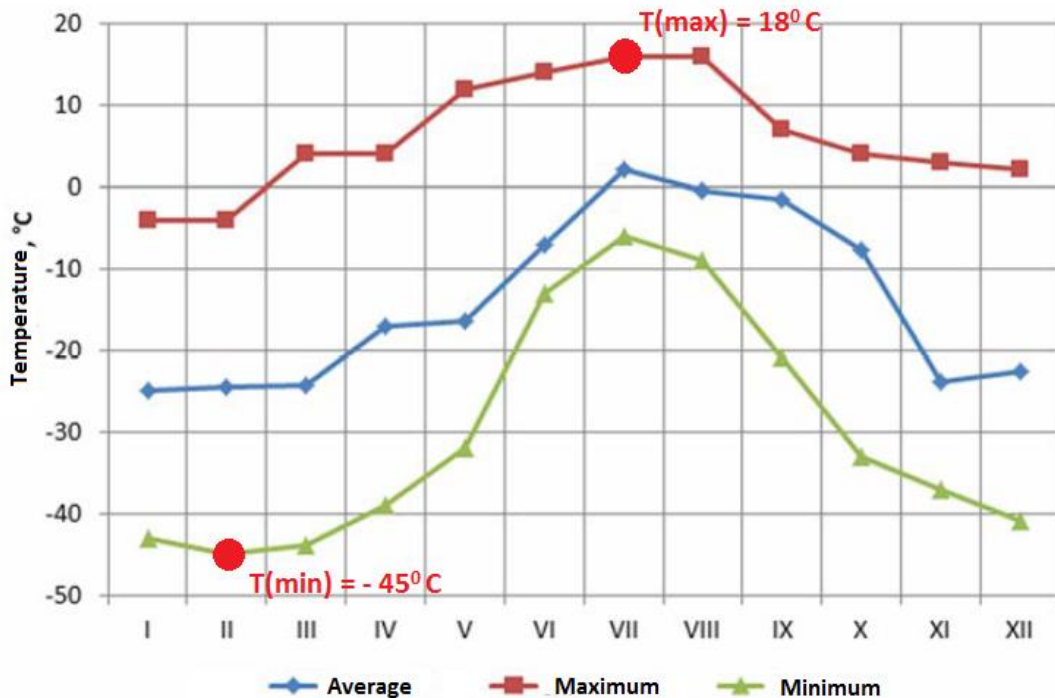


Figure 3: Annual variation of air temperature (Arctic and Antarctic Research Institute webpage, n.d.)

Average monthly wind velocities vary slightly from season to season and the annual amplitude does not exceed 2 m/s. The average annual wind velocity is less than 6 m/s (*ISO 19906, 2010*).

There are about 90 days with snowstorms during a year. The main number of blizzards is accounted for the period from October to April. In the summer, there is no more than 1 day with snowstorms per month. The average duration of blizzards is more than 900 hours per year. Prevailing direction of wind in the area is northwest – southeast (*ISO 19906, 2010*).

2.2.2. Hydrologic characteristics

According to Gazprom Neft PJSC data, water depth in the area varies in the range from 20 m in the south-west to 100 m in the north-east. The continental slope begins at the northern boundary of the license area.

1) Water temperature

The East Siberian Sea is the coldest of all the seas of the Russian Arctic. Due to some peculiarities of the spatial structure of the ice cover front position in August – September, the zonal location of the isotherms is characteristic. Along the whole coastal line, average temperatures range from +1°C to +2°C, decreasing to the northern boundary of the sea to -1°C to +0.5°C. (*ISO 19906, 2010*)

The temperature at a depth of 40 m varies in a narrow range of only -1.5°C to -1.6°C in summer and from -1.65°C to -1.80°C in winter. From this, it can be concluded that the influence of heat flow from rivers is not traced at depths of 30-40 m (*ISO 19906, 2010*).

The average sea water temperatures in the surface layer are from -1.75°C to -1°C in the winter and summer seasons, respectively. The average values of sea water temperature at a depth of 40 m are about -1.5°C (*The unified state information system webpage, n.d.*).

2) Salinity

Talking about the salinity distribution in the sea, it should be noted that there is an extensive freshening area in the western part (with salinity 17 – 22‰ in the summer and 20 – 26‰ in winter) caused by the additional influence of river waters coming from the Laptev Sea. When moving in the north and east direction, the salinity of the surface layer decreases rapidly. At the periphery, it reaches more than 28-29 ‰ during summer season and 30-31 ‰ in winter (*ISO 19906, 2010*).

The structure of the salinity fields beyond the upper mixed layer has a fairly homogeneous character. Therefore, salinity at a depth of 40 m in the East Siberian Sea varies in a narrow range from 31.2‰ to 32.8‰, both in summer and in winter (*ISO 19906, 2010*).

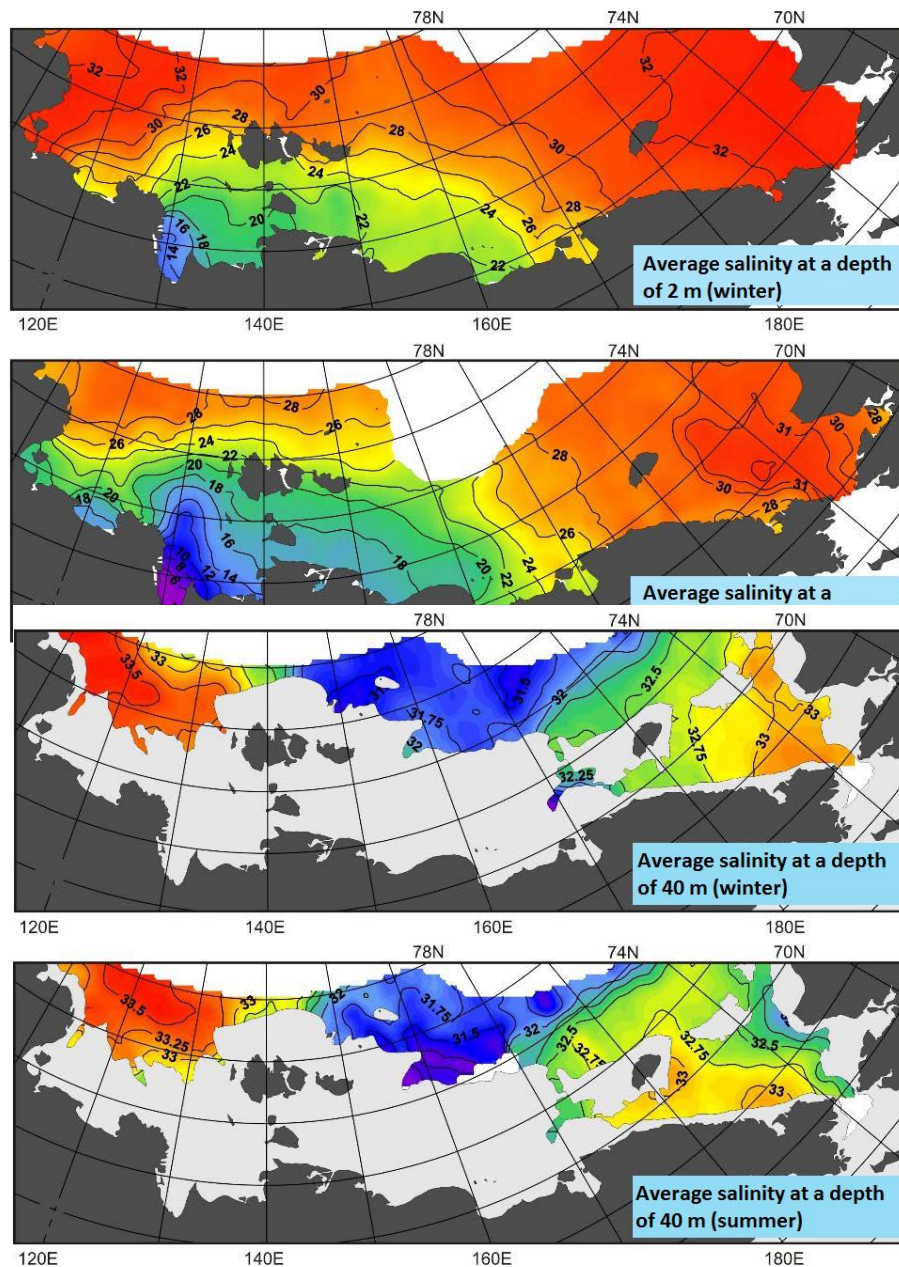


Figure 4: Distribution of salinity at the surface and at a depth of 40 m in the seas of the eastern sector of the Russian Arctic during the winter and summer period (Sea Surface Salinity Remote Sensing at CATDS Ocean Salinity Expert Center webpage, n.d.)

3) Current

Siberian alongshore current is fed by the flow of Indigirka and Kolyma rivers and continues to the Long Strait. As the averaged results of the calculations show, the current forms a water circulation before the Long Strait. Further, it sharply turns to the north and goes to the Central Arctic basin along Wrangel Island, where it joins the Transarctic Current (ISO 19906, 2010).

Non-periodic currents in the surface layer reach values of 2 – 5 cm/s. Maximum peak values of current velocities in the surface layer can reach 60 – 70 cm / s. Maximum velocities of summary currents are normally 50 – 80 cm/s (Arctic and Antarctic Research Institute webpage, n.d.).

2.2.3. Wave conditions

The East Siberian Sea disturbance is poorly developed in comparison with other seas of the Arctic Ocean due to its considerable ice cover and shallow water. From July to September, as ice edge retreats northward, the frequency of strong waves increases reaching a maximum in September (*ISO 19906, 2010*).

In the middle of August, a relatively large ice-free water area appears in the western part of the sea. Strong waves up to 4 m height can be developed there at the velocity of northwestern wind of 20 m/s. At northeast winds, the wave height does not exceed 2.5 m (*ISO 19906, 2010*).

During the ice-free period (August-September), the average values of wave heights frequency are as follows:

- 1 m – 61%;
- 1-2 m – 19%;
- 2-3 m – 15%;
- 3-5 m – 5%. (*Palmer et al., 2013*)

Table 1: 1/100 yr sea disturbance parameters (*Palmer et al., 2013*)

Parameter		Value
1/100 yr wave height	$h_{3\%}$, m	8.4
	$h_{0.1\%}$, m	11.9
1/100 yr wave period	$\tau_{3\%}$, s	6.1
	$\tau_{0.1\%}$, s	6.6

2.2.4. Ice conditions

Steady ice formation begins on the northern border of the East Siberian Sea in the area of solid ice on August 25-30. The ice edge moves to the south during September. On October 5, young ice begins to form in the coastal zone (*ISO 19906, 2010*).

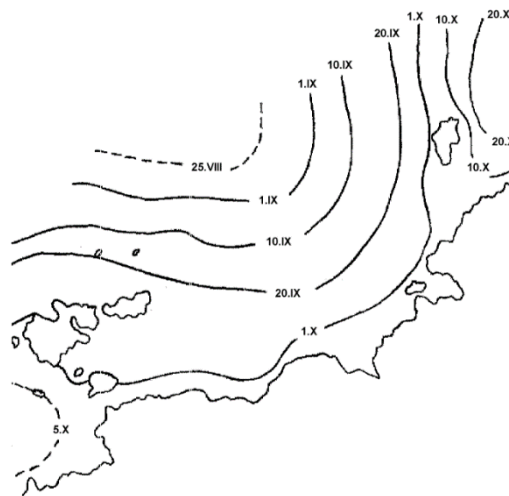


Figure 5: Isochrone lines of stable ice formation (*Arctic and Antarctic Research Institute webpage, n.d.*)

In the East Siberian Sea, fast ice is the most extensive among all the seas of Arctic Ocean (an average of 274.5 thousand km²). About 2/3 fast ice is located in the western part of the sea. This is largely facilitated by the shallow water depth (less than 25 m depths occupy 56% of the total area). Fast ice reaches its maximum development in April (sometimes in May). (*ISO 19906, 2010*)

Table 2: Ice conditions in the East-Siberian Sea during a year (*ISO 19906, 2010*)

Period	Ice conditions
October – June	The sea is completely covered with ice.
July – September	Ice cover is destroyed and the sea cleared of ice under the influence of thermal and dynamic processes.

Ice cover grows until the end of May. On June 1-5, the first signs of ice melting in the coastal zone appear. They extend to the northern regions of the sea by the mid-month. (*ISO 19906, 2010*)

Table 3: The average distribution of ice of different ages at the end of ice growth period (*ISO 19906, 2010*)

Type of ice	Distribution
One-year thick ice (more than 120 cm thick)	This ice covers about 80% of the western part of the sea and about 65% of the eastern part.
One-year thin ice (70-120 cm thick)	It represents a small part of the ice cover.
Old ice (two-year and multi-year)	The ice normally enters the sea from the Arctic basin. According to long-term data, old ice occupies an average of 12% in the western and 30% in the eastern part of the sea.

For most of the year, the ice inwash from the Arctic Basin is dominant. Due to ice drift, ice ridging in the sea is about 2-3 points depending on the particular location (it is maximum in the fast-ice border zone) (*ISO 19906, 2010*).

In the period July 5-25, fast ice is gradually destroyed. Packed ice (7-10 points) is localized in two ice massifs – Novosibirsk (in the western part of the sea) and in Ayonsky (in the eastern part). The Novosibirsk ice massif is less stable. It disappears completely at the end of September in 50% of cases (*ISO 19906, 2010*).

Table 4: Generalization of the ice conditions in the East Siberian Sea (*ISO 19906, 2010*)

Characteristic	Parameter	Av. and max values of the parameters	
		Western part	Eastern part
Ice phases	Date of the first ice appearance	During the whole year in the north Oct 1-3 – near the coastal line	During the whole year in the north Oct 3-5 – near the coastal line
	Date of fast ice appearance	Oct 15-25	Oct 25-30
	Date of fast ice breaking	July 20-25	July 10-15
	Date of ice disappearance	Do not disappear	Do not disappear
	The duration of ice season (days)	365	365
One-year ice, m	Fast ice thickness	1.9 – 2.1	1.5 – 1.9
	Length of ice fields	10000 – 15000	5000 – 10000
	Thickness of ice fields	1.4 – 1.6	2.0 – 2.4 (the northern part) 1.6 – 1.8

2.2.4.1. Physical and mechanical properties of the ice

Table 5: The mechanical characteristics of the sea ice (*ISO 19906, 2010*)

Month	Flexural strength, MPa		Compressive strength, MPa	
	Level one-year sea ice	Multi-year ice	Level one-year sea ice	Multi-year ice
September	0.18	0.33	1.13	2.42
October	0.43	0.53	3.00	3.36
November	0.61	0.65	3.63	3.73
December	0.67	0.69	3.77	3.82
January	0.65	0.67	3.74	3.77
February	0.71	0.72	3.86	3.88
March	0.70	0.70	3.84	3.85
April	0.63	0.64	3.68	3.69
May	0.50	0.50	3.26	3.26
June	0.26	0.26	1.96	1.96

The ice density varies in the range of $877 \div 890 \text{ kg/m}^3$ (*ISO 19906, 2010*).

2.2.4.2. Ice drift

Table 6: Ice Drift (*Arctic and Antarctic Research Institute webpage, n.d.*)

Season	Prevailing direction of drift		Extreme drift velocity		Average resultant vector of drift	
	In repeatability	In velocity	Prevailing direction	Other directions	Direction	Velocity
Early winter	N	NW	From 0.3-0.6 m/s (1/1 yr) to 0.6-1.1 m/s (1/100 yr)	From 0.2-0.5 m/s (1/1 yr) to 0.5-0.9 m/s (1/100 yr)	NNW	0.05 m/s
Midwinter	WNW	WNW	From 0.4-0.7 m/s (1/1 yr) to 0.7-1.4 m/s (1/100 yr)	From 0.2-0.4 m/s (1/1 yr) to 0.4-0.7 m/s (1/100 yr)	NW	0.05 m/s
Late winter	W, N	W, N, NE	From 0.3-0.4 m/s (1/1 yr) to 0.5-0.8 m/s (1/100 yr)	From 0.1-0.2 m/s (1/1 yr) to 0.2-0.4 m/s (1/100 yr)	NNW	0.03 m/s
Summer	NW	NW, S, SW	From 0.4-0.5 m/s (1/1 yr) to 0.8-1.1 m/s (1/100 yr)	From 0.2-0.3 m/s (1/1 yr) to 0.4-0.6 m/s (1/100 yr)	NW	0.02 m/s

2.2.4.3. Ice-free period

The maximum duration of ice-free period is 74 days. The average duration is 48 days (*ISO 19906, 2010*).

2.2.4.4. Icebergs

Sources of icebergs in the water area of Novosibirsk Islands are represented by “local” glaciers and icebergs coming from the other areas.

According to the Arctic Iceberg Atlas, the major local source of icebergs in the East Siberian Sea is De Long Islands. Three of the five islands have small glacier caps. However icebergs can probably be calved from the glaciers of Bennett and Henrietta Islands (*Abramov, 1996*).

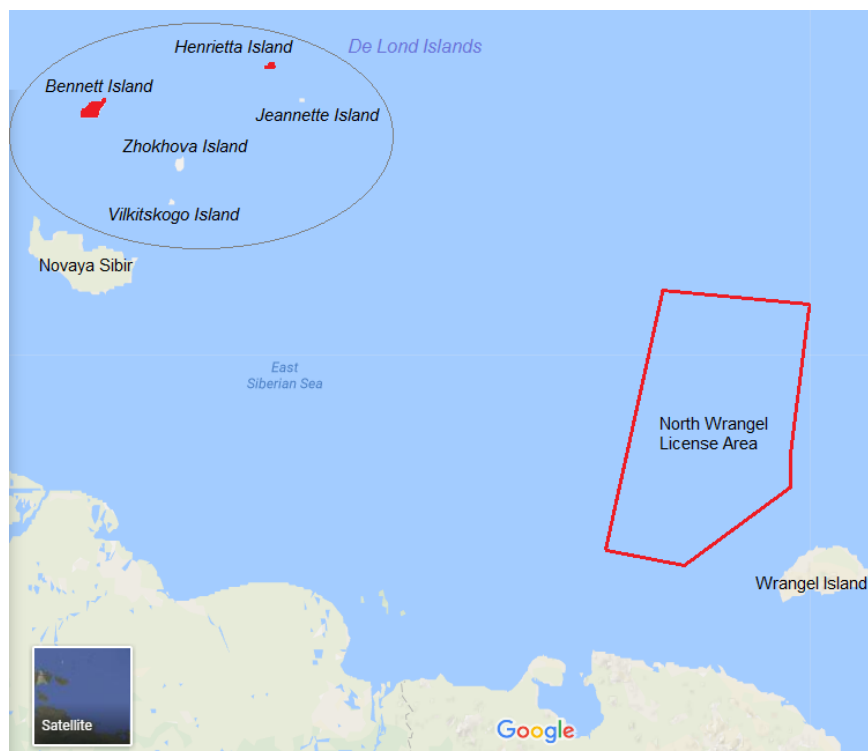


Figure 6: De Long Islands

Iceberg runoff from the glaciers of De Long Islands is very small and is estimated at 0.007 km³ that is equivalent to several large icebergs. The entry of icebergs is also possible from the central Arctic basin, as well as the Canadian sector (*Abramov, 1996*).

The total number of icebergs detected in the East Siberian Sea is small. The data were obtained from aerial observations performed in the area from 1950 to 1991 (42 years). A total of 191 flights were carried out and 1213 icebergs were recorded (*Arctic and Antarctic Research Institute webpage, n.d.*).

Icebergs appearance in the sea is most probable in March-June. From October to February, icebergs were practically not observed (*Abramov, 1996*).

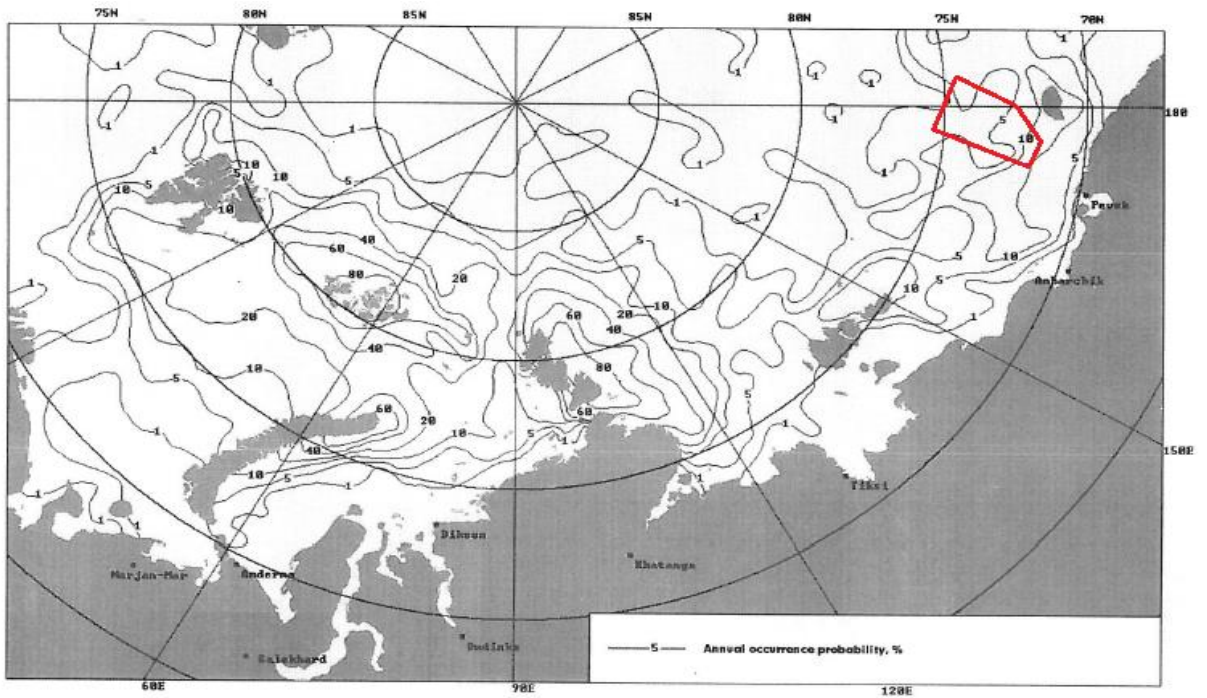


Figure 7: Annual probability of occurrence of icebergs (Abramov, 1996)

Iceberg sizes in the East Siberian Sea are relatively small. Based on the calculations obtained for other regions, it is possible to estimate in advance the maximum possible sizes of icebergs in the sea:

- a width of the order of 85 m;
- a length of not more than 150 m;
- a thickness of the order of 4-5 m (ISO 19906, 2010).



Figure 8: Glacier cap of Bennett Island (Wikimapia webpage, n.d.)



Figure 9: Iceberg in the East Siberian Sea (About Planet webpage, n.d.)

Based on the observations, it was estimated that bergy bite is the most probable (88.24%) type of icebergs in terms of occurrence in the East Siberian Sea (Abramov, 1996).

2.3. Reserves primary evaluation

The state of geological and geophysical exploration of the East Siberian Sea is extremely weak and heterogeneous. Only small-scale gravimagnetic surveys have been performed here and several seismic profiles have been worked out. Data on deep drilling are available only for the foreign part of the Chukchi Sea water area. Geophysical information is partly supplemented by the results of geological studies carried out on the island and continental land. However, the incompleteness of these observations did not allow the creation of a generally accepted model of the geological structure and evolution of the region (Gazprom Neft Shelf LLC, 2018).

The expected recoverable oil and gas resources have been evaluated at a level of more than 22.8 bboe (according to 2D seismic survey - the primary data of magnetic and gravity measurements) (Fadeev, 2015).

For the moment, 4842 linear km of 2D seismic are performed in the license area. In the coming years, the following exploration activities are planned:

- 2D seismic – 37 000 linear km;
- 3D seismic – 1 000 km²;
- Exploratory drilling – 2 wells (Fadeev, 2015).

2.4. Infrastructure

The East Siberian Sea coast is almost uninhabited. The nearest seaport with deepwater berths is located in the city of Pevek, 180 km south-west of the North-Wrangel license area (*Pevek City District webpage, n.d.*).

Severe nature limits but does not exclude the possibility of economic use of the East Siberian Sea. The main direction of economic activity there is sea transportation.

Sea Ports. Pevek is the northernmost seaport of Russia. The city also has an airport. In addition to Pevek Strait, Bay of Ambarchik is industrially used. It is located at the south-eastern coast of the East Siberian Sea between Cape Stolbovoy and Cape Medvezhy. The width of the bay at the entrance is 7 km. The depth is around 4 m.

At 350 km to the south-east of the site is located the village. Cape Schmidt, where there is a seaport and airport (*Pevek City District webpage, n.d.*).

Shipping. The license area is located near the Northern Sea Route, which runs along the Arctic coast from the Kara Strait to the Bering Strait. Parts of the route are free of ice in summer for ca. two months. The probability of navigation in the license area is low. Due to harsh ice conditions, fishing is not carried out there (*Federal Agency of Sea and River Transport webpage, n.d.*).

2.5. Limiting factors analysis

A factor that imposes certain barriers for the field development activities is considered to be a limiting one. Such factors include the following for the North Wrangel license area:

- 1) Lack of statistical data and observations in the area.
- 2) Not enough experience of the development activities in a region characterized by very severe environmental conditions.
- 3) Economic concerns.
- 4) Lack of oil and gas production and transportation infrastructure.
- 5) Significant remoteness of the license area from the mainland.
- 6) Location of the license area is adjacent to the Special Protected Natural Area (SPNA) on Wrangel Island. That will be a reason for increased attention to any field and construction work.
- 7) The presence of icebergs influences the structure design – it should be tremendous in order to withstand a possible collision.
- 8) Water depth limitations.

Although these limiting factors are very critical and can make the field development almost impossible, it is felt that conceptual study including basic

mathematical analysis of the environmental forces impact on the structure is valuable in terms of exercising and strategic planning.

3. Estimation of environmental loads on the structure

In this chapter, the environmental loads on monopod gravity-based structure are to be analyzed. These loads are created by waves, sea ice and icebergs.

Although iceberg loading is considered to cause the most negative effect on the structure integrity, all necessary calculations are to be performed in order to prove or disprove that.

3.1. Wave loads

It goes without saying, that the structure should be massive enough to withstand the severe environmental conditions of the East Siberian Sea. Based on the best practices of the structure type selection in the Grand Banks (Canada), the diameter (D) was assumed equal to 100 m. In the calculations, the GBS will be considered as a cylinder and referred to large volume structures. The term “large volume structure” is used for offshore structures with dimensions D on the same order of magnitude as typical wave lengths λ of ocean waves exciting the structure, usually $D > \lambda/6$ {in the considered case $100 \text{ m} > 11.33 \text{ m} (68/6)$ } (*DNV-RP-C205, 2010*).

Table 7: Input data for wave load calculation

Parameter	Water Depth, d			Unit
	30.00	50.00	85.00	
Max wave height, H_{max} ($H1/100$)	11.90			m
Significant wave height, H_s (for conservative design)	6.40			m
Surface, ζ_0	3.20			m
Peak wave period, T	6.60			s
Wave length corresponding to T , λ	67.55	68.03	68.05	m
Angular frequency, ω	0.95			s^{-1}
Wave number, k	0.0935	0.0928	0.0927	-
d/λ	0.44	0.73	1.25	-
	Intermediate water depth	Deep water	Deep water	
Characteristic dimension, D	100.00			m

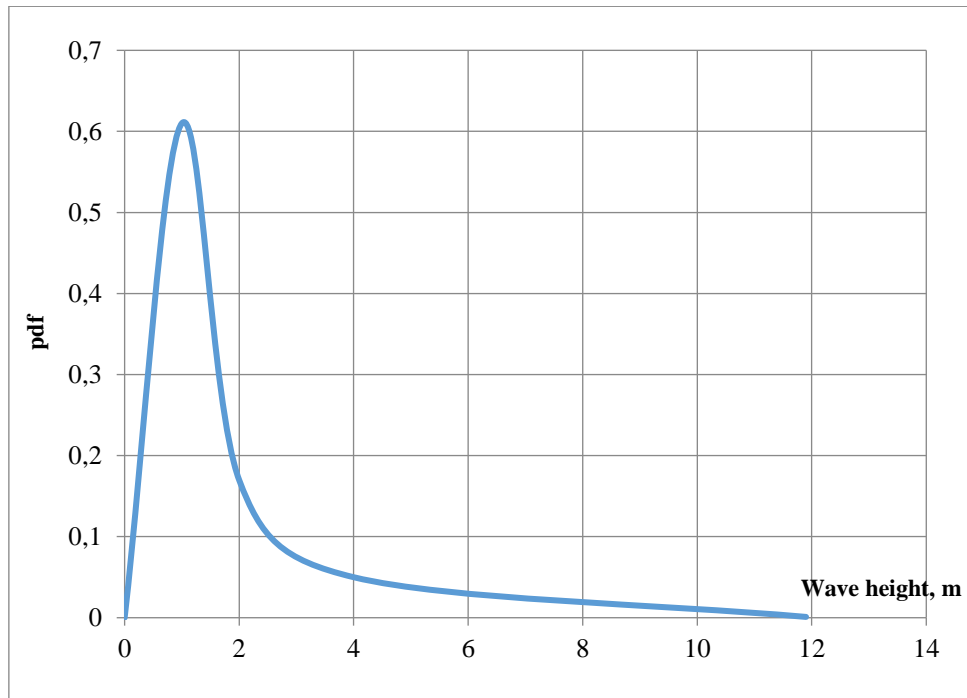


Figure 10: Wave height probability distribution for East Siberian Sea (Palmer et al., 2013)

The analysis of wave loads is to be carried out for the zones of the North Wrangel license area characterized by different water depth: 30 m, 50 m and 85 m.

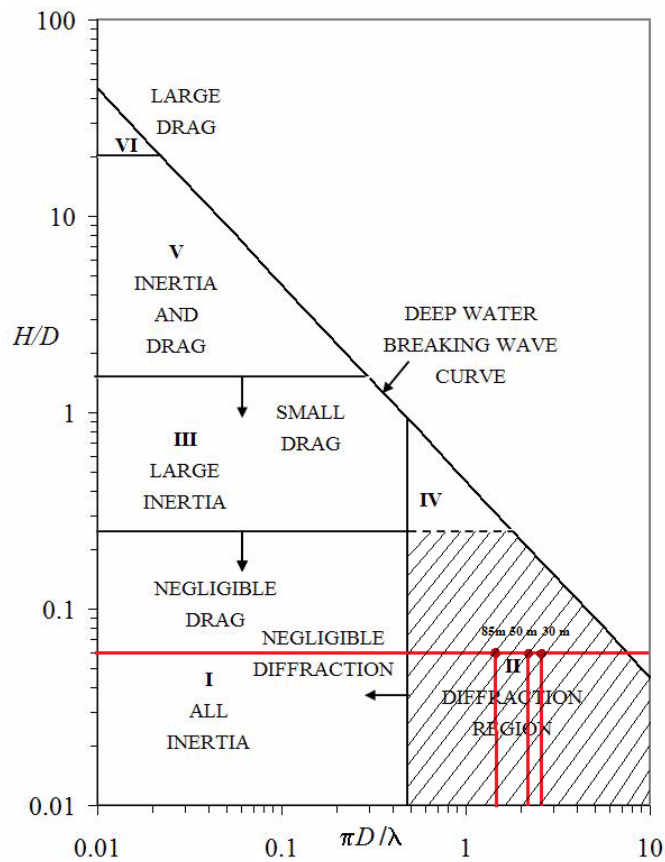


Figure 11: Different wave force regimes (Chakrabarti, 1987) (DNV-RP-C205, 2010)

In order to determine what force regime shall be implemented for describing the interaction between the structure and wave loading, it is necessary to estimate the relations H/D and $\pi D/\lambda$ for each water depth and check the diagram illustrated below.

Table 8: Force regime determination

Parameter	30 m	50 m	85 m
H/D	0.06	0.06	0.06
$\pi D/\lambda$	2.77	2.15	1.65

It is well seen that the case corresponds to diffraction (reflection) wave force regime meaning that the wave condition is dominated by inertia forces (*DNV-RP-C205, 2010*).

An assumption about a quasi-static response of the structure in the operational mode is made here. In this case, deterministic approach is sufficient for the calculations (*International Ship and Offshore Structures Congress, 2012*).

According to DNV-RP-C205, wave-induced loads on large volume structures can be predicted based on potential theory which means that the loads are deduced from a velocity potential of the irrotational motion of an incompressible and inviscid fluid (*DNV-RP-C205, 2010*).

3.1.1. Theoretical basis for wave loads calculation

Due to reflected waves, the theoretical basis will be represented by MacCamy & Fuchs theory for cylinder in ideal fluid that takes into account the diffraction effects.

For the large cylinder we must look at the incoming potential φ_i and the reflected (or diffracted) potential φ_d :

$$\varphi = \varphi_i + \varphi_d \quad (1)$$

The conditions to be satisfied are expressed by the following set of equations:

$$\nabla^2 \varphi = 0 \quad - \text{in the fluid} \quad (2)$$

$$\frac{\partial \varphi}{\partial r} = 0 \quad - \text{on the cylinder} \quad (3)$$

$$\frac{\partial^2 \varphi}{\partial t^2} + g \frac{\partial \varphi}{\partial z} = 0 \quad \text{at } z = 0 \quad - \text{the linearized surface condition} \quad (4)$$

$$\frac{\partial \varphi}{\partial t} = 0 \quad \text{at } z = -d \quad - \text{the sea bottom} \quad (5)$$

φ_d creates reflected wave going away from the cylinder.

Incoming potential is expressed as:

$$\varphi_i = \frac{\xi_0 g}{\omega} \cdot \frac{\cosh(k(z+d))}{\cosh(kd)} \cdot e^{i(kx - \omega t)} \quad (6)$$

$$\frac{\omega^2}{gk} = \tanh(kd) \quad (7)$$

The term $e^{i(kx-\omega t)}$ has real physical meaning. It is understood that the actual potential is the real part of this complex expression (MacCamy, 1954).

As the body is a cylinder $\varphi_d \sim \psi(r, \theta, t)$; i.e. we should use cylinder coordinates. Furthermore, the z-dependency in the incoming wave would appear also in the reflected wave. Thus:

$$\varphi_d = \cosh(k(z+d)) \cdot \psi(r, \theta, t) \quad (8)$$

where ψ is given in cylindrical coordinates.

Since $\nabla^2 \varphi_i = 0$, we must have $\nabla^2 \varphi_d = 0$. By using separation of variables, we obtain:

$$\psi(r, \theta, t) = R(r)\Theta(\theta)T(t) \quad (9)$$

$$\text{Then, the potential will be: } \varphi_d = \cosh \cdot k(z+d)R(r)\Theta(\theta)T(t) \quad (10)$$

After calculating the values of $R(r)$, $\Theta(\theta)$ and $T(t)$, the potential φ_d is known. Therefore, we have a solution for the total potential φ . From this the expressions for pressure and force can be easily found (Gudmestad, 2015).

The force per unit length can be written as:

$$f = C_M \rho_w \frac{\pi D^2}{4} a_x|_{x=0} \quad (11)$$

where C_M is mass coefficient, ρ_w – sea water density, D – structure's diameter and $a_x|_{x=0}$ – acceleration.

The obtained formula looks exactly the same as the one for mass force. However, the fundamental difference is that here the expression for C_M is a complex mathematical term depending on the ratio D/L (Gudmestad, 2015).

The acceleration a_x is computed according to the formula below:

$$a_x|_{x=0} = \xi_0 g k \frac{\cosh(k(z+d))}{\cosh(kd)} \cos(\omega t) \quad (12)$$

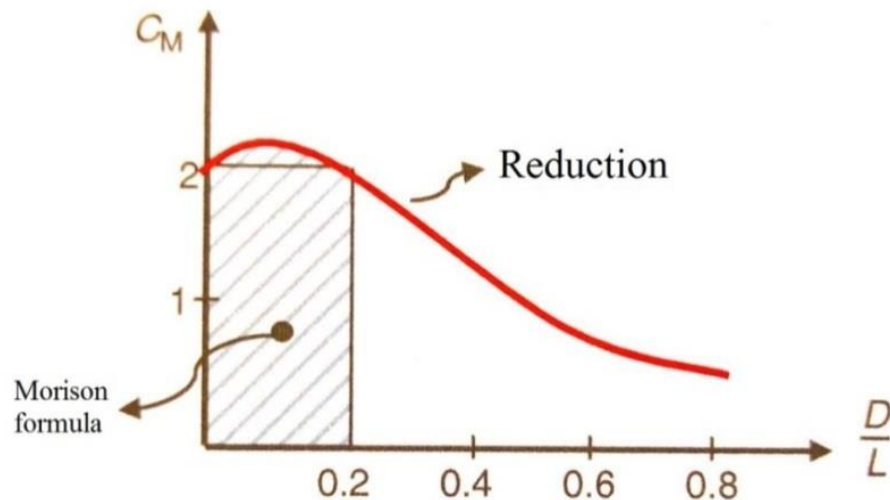


Figure 12: The relation between C_M and D/L (Gudmestad, 2015)

3.1.2. Calculation of wave load on the offshore structures

Due to an assumption about quasi-static response of the structure, for carrying out the deterministic calculations it is permissible to use Excel software.

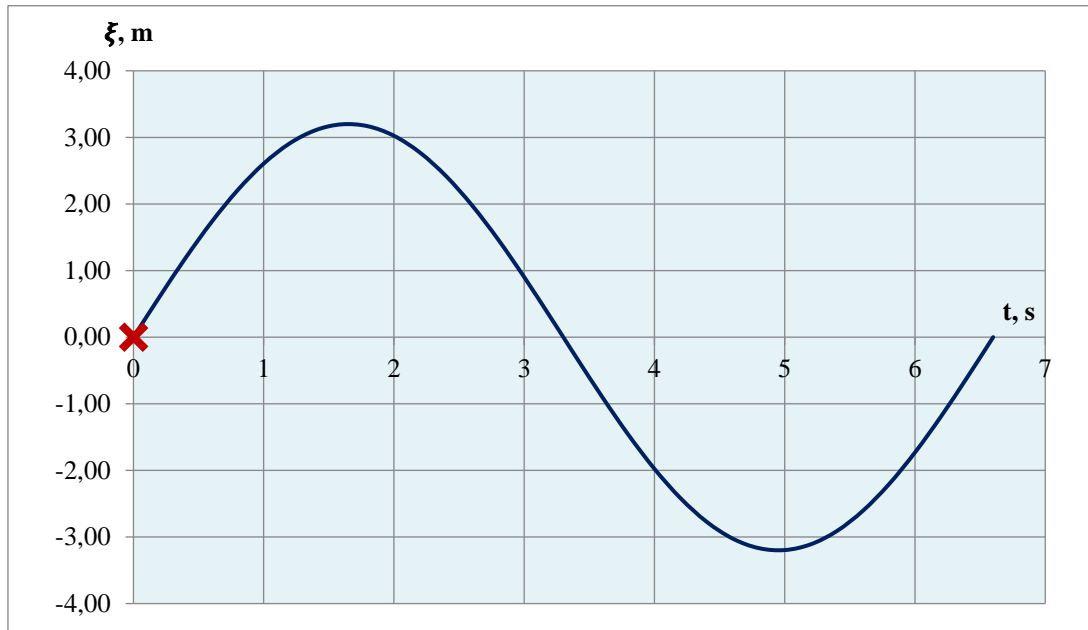


Figure 13: Wave profile

Let us take the time moment $t = 0$ s.

Considering wave loads on large offshore structures we suppose that the wave condition is totally dominated by inertia force. In order to provide the design basis with sufficient safety level, it is necessary to calculate the load based on the maximum possible inertia forces that reach its peak value in the area where wave passes still water level.

Total inertia force is normally computed in the following way:

$$F = \int_{-d}^{\xi} f(z) dz \quad (13)$$

Since Excel is not able to calculate integrals, we have to apply another technique. In this case, we integrate from bottom to still water level by using the basic definition of integration – area under the graph of function $f(z)$. Here we approximate the area of function by dividing the space into rectangles and adding the areas.

The results of total inertia force estimation for the different zones of the North Wrangel license area characterized by different water depths are given in the table below.

Table 9: The results of inertia force calculation

Parameter	Water depth, d			Unit
	30	50	85	m
Total inertia force	100.64	103.45	104.75	MN

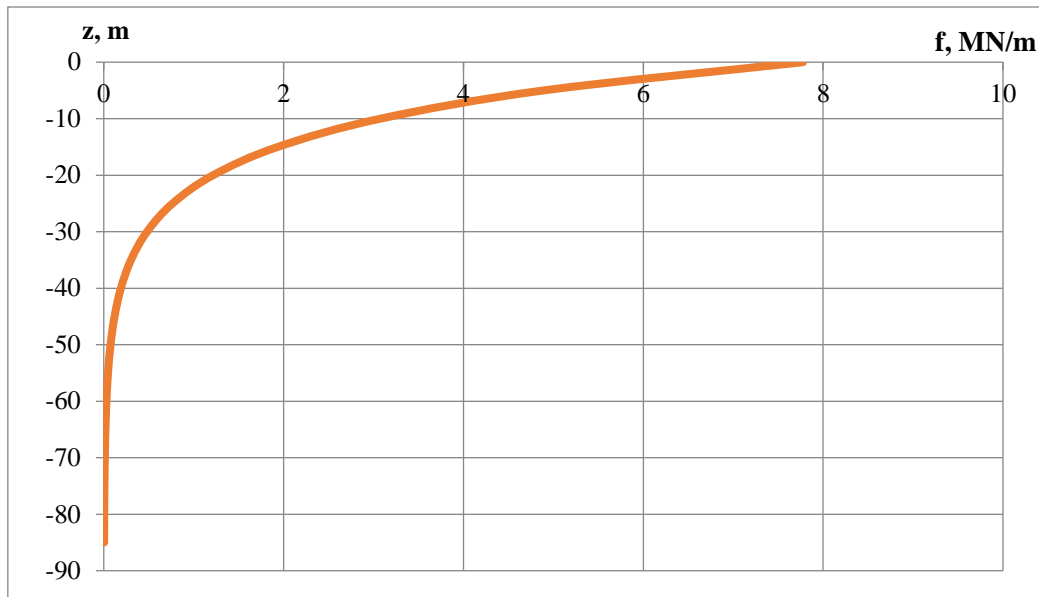


Figure 14: Inertia force distribution along the structure ($d=85$ m)

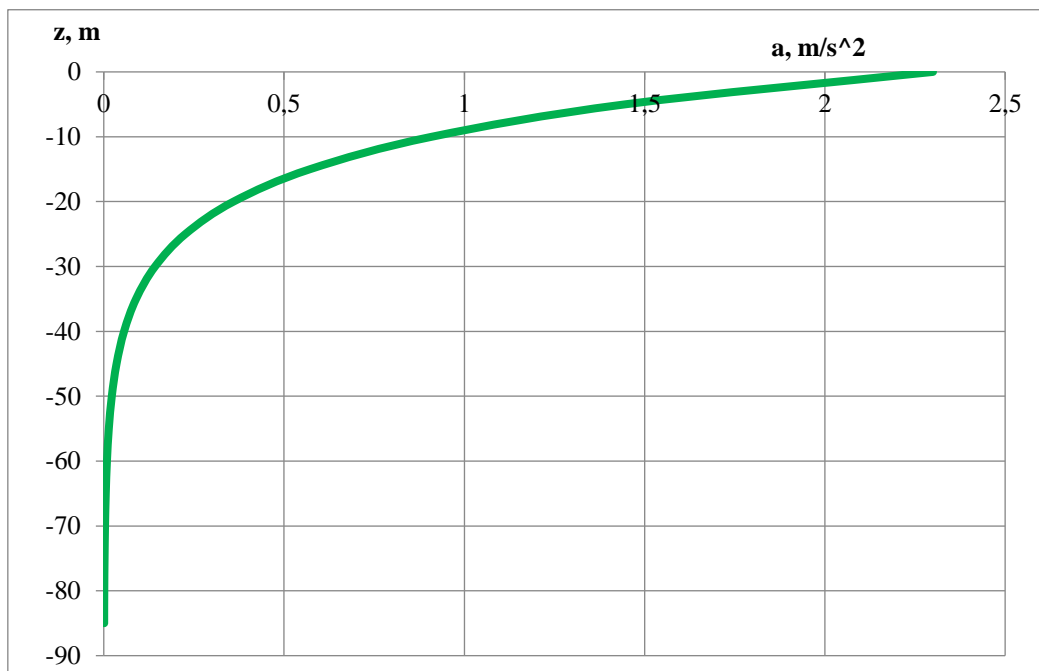


Figure 15: Acceleration vs. depth ($d=85$ m)

The distributions have the same shape for the structures installed at water depth of 30 m and 50 m.

3.2. Ice loads

The East Siberian Sea is covered with ice during the period of more than 10 months (*Arctic and Antarctic Research Institute webpage, n.d.*). It is unofficially recognized as the “iciest” sea in the Arctic. Obviously, it is the ice loads that create the most significant environmental impact on the structure, which can potentially be installed in the area.

The following sea ice types occur in the North Wrangel license area at the end of the growth period:

- One-year thin ice (0.7-1.2 m thick);
- One-year thick ice (more than 1.2 m thick);
- Old ice (up to 2.4 m thick) (*Arctic and Antarctic Research Institute webpage, n.d.*).

Multi-year ice will cause much bigger ice loads and is able to create massive rubble accumulation around the structure. That is what one should be aware of when making a design basis.

The gravity-based structures subjected to the analysis are of vertical wall and sloping wall configurations.

3.2.1. Theoretical basis for ice loads calculation

The limit stress approach will be implemented for estimation of drift ice loads on both vertical and sloping walls. This scenario controls the maximum possible action and corresponds to the situation when the stresses reach some limit values (*Løset et al., 2006*).

Depending on the wall profile, a failure mode of ice and, consequently, the loads will be different. In the considered case, a sloping wall structure experiences less ice loads because ice is broken by bending. Since compressive strength of ice is normally higher than flexural strength, the structure with vertical wall profile is subject to relatively huge ice load near the waterline (crushing failure mode). However, a sloping wall concept is challenged by rubble accumulation on the structure surface. This rubble is pushed along the surface by ice sheet and induces additional ice actions due to its weight and friction forces (*Løset et al., 2006*).

1) Vertical structure

According limit stress scenario, level ice actions (normal stress) on the structure with vertical walls can be estimated by using Korzhavin's formula generally used in many codes and regulations:

$$F = I \cdot K \cdot m \cdot \sigma_C \cdot D \cdot h \quad (14)$$

where:

I – indentation factor;

K – contact factor;

m – plane shape factor;

σ_C – unconfined compressive strength of ice;

D – structure's diameter;

h – ice thickness (*Løset et al., 2006*).

Indentation factor takes into account the crystallographic structure of the ice, its properties, the correlation between the structure's diameter and the ice thickness, the influence of the stress/strain field on strength. For floating ice covers (columnar structure of ice), the factor I varies between 3 and 4.5 (Løset *et al.*, 2006).

Contact factor K describes the imperfect contact between an ice sheet and the structure. It may be in the range of 0.02 – 0.13 (Løset *et al.*, 2006).

Plane shape factor varies in narrow limits between 0.9–1.0 where 0.9 corresponds to a cylinder and 1.0 to a flat contact surface (Løset *et al.*, 2006).

2) Sloping structure

According to Croasdale 2D loading model based on analysis of a semi-infinite elastic beam on an elastic foundation, the equation for the horizontal component of load, that is needed to push broken ice up along the sloping surface, can be written in the following way:

$$F_H = C_1 \cdot \sigma_f \cdot D \cdot \left[\frac{\rho_w \cdot g \cdot h^5}{E} \right]^{0.25} + z \cdot h \cdot \rho_i \cdot g \cdot C_2 \quad (15)$$

where:

C_1, C_2 – coefficients depending on the wall inclination and dynamic friction;

σ_f – flexural strength of ice;

D – structure's diameter;

ρ_w, ρ_i – water and ice densities;

h – ice thickness;

E – Young's modulus;

z – height of rubble on the structure's slope (Løset *et al.*, 2006).

The first term in the equation represents the action due to flexural failure of the advancing ice sheet. The second term represents the action due to ride-up of the broken ice pieces. The coefficients C_1 and C_2 are given by:

$$C_1 = 0.68 \frac{\xi_1}{\xi_2} \quad (16)$$

$$C_2 = \xi_1 \left(\frac{\xi_1}{\xi_2} + ctg\alpha \right) \quad (17)$$

where:

$$\xi_1 = \sin\alpha + \mu \cdot \cos\alpha \quad (18)$$

$$\xi_2 = \cos\alpha - \mu \cdot \sin\alpha \quad (19)$$

where:

α – slope angle;

μ – coefficient of the ice dynamic friction over the structure surface (Løset *et al.*, 2006).

3.2.2. Estimation of ice loads on vertical structure and sloping structure

As it has already been mentioned above, ice loads on the structure in the North Wrangel license area is a very critical parameter. In addition, when estimating these loads, an analyst operates in the environment characterized by relatively significant lack of statistical data and big uncertainties. In this regard, a deterministic approach, or so called “single-point estimate”, to the computations is not sufficient. Monte Carlo method seems to be the most optimal technique that can be implemented for this particular case.

The method has a number of advantages over traditional deterministic approach, namely:

- 1) It performs risk analysis by producing models of possible outcome values distributions;
- 2) The simulation can perform thousands of recalculations before it is complete;
- 3) It provides an excellent image of input parameters having the biggest effect on bottom-line results;
- 4) The approach contributes to understanding of exactly what inputs had which values together when certain outcomes occurred;
- 5) There is a possibility to model interdependent relationships between input variables (*Kadry, 2015*).

Since Matlab software is considered to be strong numerical computing environment, it was used for performing the simulations of ice loads.

In this subchapter, two cases are to be considered: the loads on the structure with vertical walls and sloping walls. It should be noted, that each case is accompanied by a system of assumptions needed to “fill in the gaps” associated with the lack of data, for making a particular model applicable to the design basis. As a rule, the assumptions are based on available statistics, technological considerations, best practices, data from regions characterized by similar conditions, etc.

1) Vertical structure

System of assumptions

- a) Crushing is considered as the only failure mode occurred.
- b) There is simultaneous failure development over the contact area between the ice and the structure.
- c) Unconfined compressive strength characterizes the whole stress field around the structure.
- d) The distribution of the stochastic variables' probabilities (σ_c , h , K , I) is subject to normal law.

e) The plane shape factor is a constant determined for a cylinder shaped structure.

Table 10: Input data for estimation of ice loads on the vertical structure

Parameter	Value	Unit
Structure's diameter, D	100	m
Plane shape factor, m	0.9	-
Ice thickness, h	0.7 ÷ 2.4	m
Unconfined compressive strength of ice, σ_c	1.13 ÷ 5.13	MPa
Indentation factor, I	3.0 ÷ 4.5	-
Contact factor, K	0.02 ÷ 0.13	-

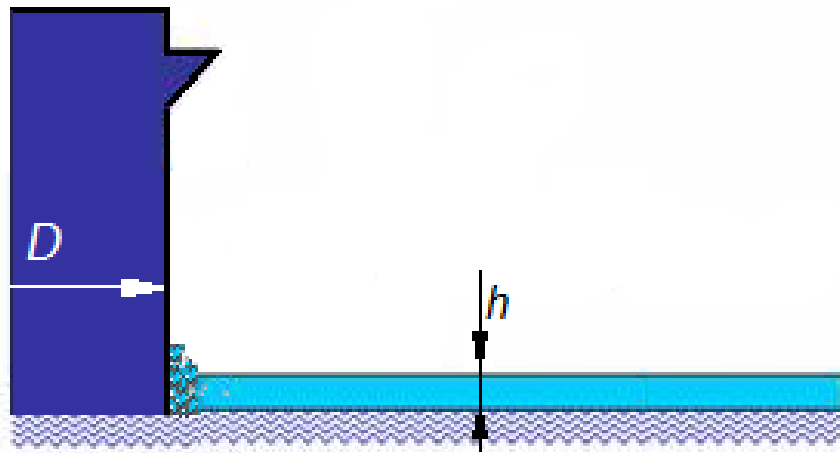


Figure 16: Ice impact on the vertical structure (Løset et al., 2006)

The simulation code and the Matlab sketches are given in the Appendix (A-1, B-1).

The simulation results are listed in the table below.

Table 11: The simulation results of ice loads on the vertical structure

Parameter	Value	Unit
Most probable ice load on the structure, F_{pr}	≈ 120	MN
The load that is possible once in 10 years, $F_{1/10}$	≈ 180	
The load that is possible once in 100 years, $F_{1/100}$	≈ 280	
The load that is possible once in 10000 years, $F_{1/10000}$	≈ 300	

2) Sloping structure

System of assumptions

- The structure width is constant at the ice interaction level.
- The situation, when the rubble near the structure breaks the ice it lies on and is further get submerged, is not considered.

c) The height of rubbles on the structure's slope is estimated in accordance with the formula used in Confederation Bridge (Canada) design due to the ice conditions similarities (Belliveau et al., 2002):

$$z = 7.6h^{0.64} \quad (20)$$

d) The distribution of the stochastic variables' probabilities (σ_f , h , z) is subject to normal law.

e) The sea ice density is taken as a constant for the whole area.

Table 12: Input data for estimation of ice loads on the sloping structure

Parameter	Value	Unit
Structure's diameter, D	120	m
Slope angle, α	60	°
Young's modulus, E	8700	MPa
Coefficient of the ice dynamic friction over the structure surface, μ	0.2	-
Sea water density, ρ_w	1023	kg/m ³
Sea ice density, ρ_i	884	kg/m ³
Gravity acceleration, g	9.81	m/s ²
Flexural strength of ice, σ_f	0.18 ÷ 0.72	MPa
Ice thickness, h	0.7 ÷ 2.4	m
Height of rubble on the structure's slope, z according to (20)	6.05 ÷ 13.31	m

The simulation code and the Matlab sketches are given in the Appendix (A-2, B-2).

The simulation results are listed in the table below.

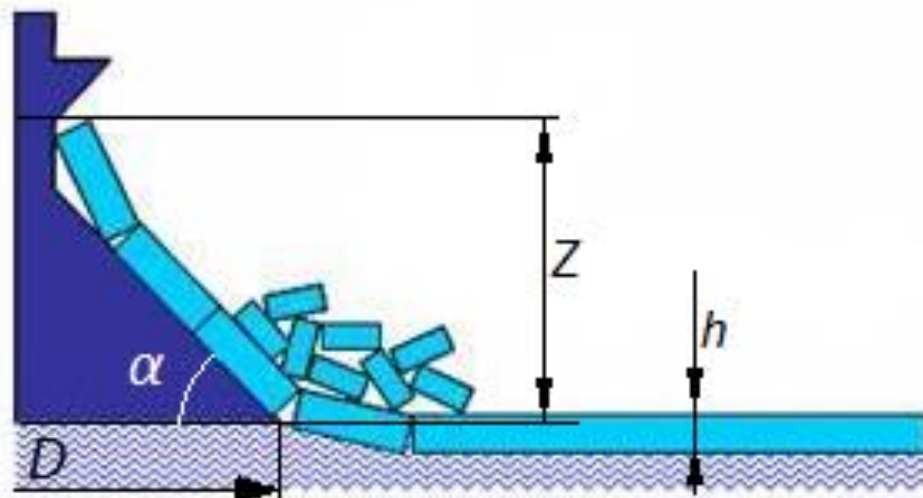


Figure 17: Ice impact on the sloping structure (rubble accumulation) (Løset et al., 2006)

Table 13: The simulation results of ice loads on the sloping structure

Parameter	Value	Unit
Most probable ice load on the structure, F_{pr}	≈ 26	MN
The load that is possible once in 10 years, $F_{1/10}$	≈ 35	
The load that is possible once in 100 years, $F_{1/100}$	≈ 42	
The load that is possible once in 10000 years, $F_{1/10000}$	≈ 49	

3.2.3. Calculation of iceberg load on cylinder structure

Iceberg load estimation is supposed to be an important design consideration. It is characterized by uncertainties caused by:

- shape and sizes of an iceberg;
- the ice properties;
- iceberg impact velocity;
- iceberg trajectory (*Sayeed et al., 2017*).

Iceberg impact force is highly dependent on the collision energy, which in turn is determined by the impact velocity between the ice mass and the structure. The velocity is largely dependent on the iceberg drift velocity at the time of impact with the structure (*Sayeed et al., 2017*).

Generally, the impact force is estimated by the following way:

$$\int_0^S F ds = \frac{1}{2} M \cdot (1 + C_m) \cdot (V_{initial}^2 - V_{final}^2) \quad (21)$$

where:

F – impact force;

s – indentation of the structure into the iceberg body;

M – mass of the iceberg;

C_m – added mass coefficient;

$V_{initial}$ – drift velocity of the iceberg;

V_{final} – drift velocity after the impact (*Løset et al., 2006*).

System of assumptions:

a) The glacier being the main source of icebergs in the area is considered to have the relatively constant thickness of the end entering water, so the icebergs' height is supposed to be constant as well.

b) The iceberg length, width and drift speed are stochastic variables and its probability densities are subject to normal law.

c) The ice density is taken as a constant value.

d) Open water model is assumed.

e) The iceberg trajectory passes the structure location.

f) The iceberg drift is considered relative to water (*Ettle, 1974*).

g) The drift is steady state (*Ettle, 1974*).

- h) Coriolis effect is neglected (*Ettle, 1974*).
- i) The drift velocity after the impact is considered to be 0.

Iceberg drift is affected by the environmental forces (i.e. wind, waves, and currents). In order to estimate the drift velocity we have to refer to the best practices because there is no any statistical data. In this particular case, the Grand Banks experience was taken as a basis.

According to the method proposed by *Ettle (1974)* for the Grand Banks iceberg drift estimation, the drag coefficient for the iceberg sail (C_{Da}) and the drag coefficient for the iceberg keel (C_{Dw}) can be compared if the iceberg's movement is considered relative to water rather than relative to the earth. Taking into account assumptions f), g) and h), it is possible to equate the drag force due to the air with the drag force due to the water, as follows (*Ettle, 1974*):

$$\frac{1}{2}\rho_a \cdot C_{Da} \cdot V_a^2 \cdot S_a = \frac{1}{2}\rho_w \cdot C_{Dw} \cdot V_{initial}^2 \cdot S_w \quad (22)$$

By rearranging, we obtain: (*Ettle, 1974*)

$$\frac{C_{Da}}{C_{Dw}} = \frac{\rho_w \cdot V_{initial}^2 \cdot S_w}{\rho_a \cdot V_a^2 \cdot S_a} \quad (23)$$

If we assume the ratio of water density to air density to be 10^3 and use 3.5 to 1.0 for the ratio of S_w to S_a , we obtain: (*Ettle, 1974*)

$$\frac{C_{Da}}{C_{Dw}} = 3.5 \cdot 10^3 \left(\frac{V_{initial}}{V_a} \right)^2 \quad (24)$$

where:

- ρ_a – density of air;
- ρ_w – density of sea water;
- C_{Da} – drag coefficient for sail;
- C_{Dw} – drag coefficient for keel;
- V_a – wind speed;
- $V_{initial}$ – iceberg drift velocity relative to water;
- S_a – cross-sectional area perpendicular to air flow;
- S_w – cross-sectional area perpendicular to water flow (*Ettle, 1974*).

Since the estimation is subject to even more uncertainties, it was performed by using Matlab software.

Table 14: Input data for estimation of ice loads on the sloping structure

Parameter	Value	Unit
Ice density, ρ_i	884	kg/m ³
Height of the iceberg, h	5	m
Added mass coefficient, C_m	0.2	-
Indentation of the structure into the	0.001	m

iceberg body, s		
Length of the iceberg, l	20 ÷ 150	m
Width of the iceberg, b	10 ÷ 85	m
Drift velocity of the iceberg, $V_{initial}$	0.173 ÷ 0.185 ^(Ette, 1974)	m/s ²

Table 15: The simulation results of iceberg load

Parameter	Value	Unit
Most probable ice load on the structure, F_{pr}	≈ 340	MN
The load that is possible once in 10 years, $F_{1/10}$	≈ 520	
The load that is possible once in 100 years, $F_{1/100}$	≈ 660	
The load that is possible once in 10000 years, $F_{1/10000}$	≈ 840	

The simulation code and distribution graphs for PDF, CFD and EDF(F) are given in the Appendix (A-3, B-3).

Table 16: The overall results of ice loads estimation

Parameter	Value			Unit
	Vertical wall	Sloping wall	Iceberg	
Most probable ice load on the structure, F_{pr}	≈ 120	≈ 26	≈ 340	MN
The load that is possible once in 10 years, $F_{1/10}$	≈ 180	≈ 35	≈ 520	
The load that is possible once in 100 years, $F_{1/100}$	≈ 280	≈ 42	≈ 660	
The load that is possible once in 10000 years, $F_{1/10000}$	≈ 300	≈ 49	≈ 840	

Due to the iceberg dimensions and drift speed, its impact forces cause the maximum loading on the structure. When considering the ice sheet load, sloping-sided structure experiences less loading due to the fact that compressive strength of ice is normally higher than flexural strength.

The structure that can potentially be installed in the license area should have the resistance exceeding the maximum possible load, i.e.

$$R > 840 \text{ MPa}$$

where R is the structure's resistance.

Ice management activities are definitely to be carried out.

4. Status of Technology

It goes without saying that current status of significant hydrocarbon reserves discoveries in the Arctic requires both well proven technologies and new advanced solutions for oil and gas field development. At the same time, this can be considered as incentive to design new offshore structures, platforms and equipment for operation in severe conditions.

However, the experience in construction and operation of oil and gas facilities in the Arctic should also be taken into account when considering different basic development concepts for a field of interest located in the East Siberian Sea.

This chapter includes analysis of the existing Arctic and sub-Arctic field development technologies and approaches implemented in the recent years by leading international and domestic companies.

The East Siberian Sea is characterized by shallow water depth with flat bottom sloping to the north-east. As it has been already stated in the previous chapter, the North Wrangel license area is characterized by the following key environmental parameters listed in the table below.

Table 17: General information for the North Wrangel license area (*ISO 19906, 2010*)

Parameter	Value
Water depth, m	30 to 85
Minimum air temperature, °C	-40 to -51
Minimum water temperature, °C	-1.8
Maximum current velocity in the surface layer, cm/s	50 to 80
1/100 yr wave height, m	11.9
Average duration of ice-free period, days	48
Average ice thickness, m	> 2
Ice ridges thickness, m	> 6
Icebergs and its fragments can be found in the area	

The following criteria were used when selecting analogies for the analysis:

- Water depth;
- Climate conditions;
- Hydrological conditions;
- Ice conditions.

It is worth noting that artificial islands being one of the solutions for the Arctic field development were not considered due to minimum water depth of the North Wrangel license area.

4.1. Pechora Sea and Sea of Okhotsk

4.1.1. “Prirazlomnoye” Project

Prirazlomnoye oil field is located on the Pechora Sea shelf in the exclusive economic zone of the Russian Federation. Currently, the project is operated by Gazprom Neft Shelf LLC.

The distance from the oil field to the nearest shore line, where Varandey settlement is located, is 58 km. At the same time, the distances to “Naryan-Mar” river port and sea port of Murmansk are 250 km and 980 km, respectively.

Climate in the considered area can be characterized as severe due to decreased influence of the warm Atlantic currents and presence of ice cover during 7-8 months a year.

The coldest months are January and February and the warmest ones are July and August. Annual average air temperature is below 0°C entirely in the region. Duration of the period with positive temperatures is ca. 130-156 days.

Water depth in the area of the platform installation varies from 19 to 21 m (*Gazprom Neft Shelf LLC, 2011*).

Hydrological regime and ice conditions of the Barents Sea are significantly influenced by a system of cold and warm ocean currents (*ISO 19906, 2010*).

Ice cover of the Pechora Sea consists of first-year ice of different thickness:

- thin first-year ice (30 – 70 cm);
- thick first-year ice (120 – 200 cm).

The thick ice appears in March in the northern part of the sea and spreads along the coastal line occupying the oil field area. In late June – early July, thick first-year ice retreats to the east (*Gazprom Neft Shelf LLC, 2011*).

The main environmental features of the area are listed in the table below.

Table 18: General information for the Pechora Sea (*ISO 19906, 2010*)

Parameter	Value
Winter Season	October to July
Summer Season	August to September
Average minimum air temperature, °C	-18 to -20
Absolute minimum air temperature, °C	-48
10 minute average wind speed, m/s	20 to 25
Significant wave height (< 100 m water depth), m	1.5 to 7.0
Near surface maximum speed of current, cm/sec	100 to 130
Average water surface salinity, ppt	25 to 33
Summer average surface water temperature, °C	+6 to +8
Winter average water temperature, °C	-1.8 to 0
Average ice-free period, days	110

First ice occurrence	20 October to 5 November
Last ice occurrence	25 June to 15 July
Level ice (first-year) thickness, m	0.7 to 1.1
Rafted ice thickness, m	0.8 to 1.0
Ridges sail height, m	3.0 to 4.0
Ridges keel depth, m	15.0 to 18.0
Stamukhi, m	< 20

According to Gazprom Neft Shelf LLC, Prirazlomnoye project has the following features:

- Recoverable reserves are estimated at the level of more than 70 million tons of oil;
- Planned rate of production is more than 6 million tons of oil a year;
- Expected reservoir life is 25 years;
- Number of wells to be drilled is 32 (*Gazprom Neft Shelf LLC, 2018*).



Figure 18: IRGBS “Prirazlomnaya” (Gazprom Neft Shelf LLC, 2013)

The Ice-Resistant Gravity Base Structure (IRGBS) “Prirazlomnaya” is used for the field development. This platform was designed to simultaneously perform the following operations: drilling, production, processing, storage and offloading.

The IRGBS is a structure of gravity type manufactured from steel and concrete (caisson type). The steel structures were designed to withstand all the loads without taking into account the influence of concrete, which is basically used to provide additional strength. The caisson has sloping-walls shape in order to effectively take up ice loads (*Gazprom Neft Shelf LLC, 2011*).

The IRGBS rests on the sea bottom without additional fastenings in the operation conditions. On-bottom stability is provided by the structure weight as well as water and concrete ballast.

Process system of the platform provides all stages of in-field oil processing. The products obtained meet all the requirements for commercial oil (*Gazprom Neft Shelf LLC, 2011*).

Oil is offloaded directly from the platform to ice resistant shuttle tankers (IRST) “Mikhail Ulyanov” and “Kirill Lavrov”. The deadweight for both tankers is 70 thousand tons each (*Gazprom Neft Shelf LLC, 2013*).

The platform was designed for year-round continuous operation with regular supply of necessary materials every 15-60 days. 200 employees work at the platform on a rotational basis (*Gazprom Neft Shelf LLC, 2011*).

4.1.2. Sakhalin Projects (on the example of Arkutun-Dagi field)

Arkutun-Dagi oil and gas field is located in the northeast of Sakhalin-Island on the continental shelf of the Sea of Okhotsk ca. 25 km from the shore. Field development activities are being organized within the framework of Sakhalin-I project (*Neftegaz.RU webpage, n.d.*).

Generally, northeastern Sakhalin coast is characterized by harsh climatic conditions that make it challenging to implement oil and gas projects and require special engineering solutions for ensuring technological and environmental safety (*Gudmestad et. al., 2000*).

Striking feature of the northeastern Sakhalin shelf climate, especially in the area of Arkutun-Dagi field, is monsoon air circulation. It is one of the reasons why cold and long winter seasons are typical for the major part of the Sea of Okhotsk. This fact allows describing marine climate of the sea as Arctic type climate (*ISO 19906, 2010*).

Maximum wind speed is mainly observed in the cold season (November – January) and during the passage of deep cyclones and typhoons.

Relative humidity in the area is very high throughout a year. Snow cover normally lasts up to 200 days. Snowstorms occur quite often during passage of cyclones. In the period from October to May, sheet of glaze and icing of marine structures and oil and gas facilities are possible (*Gudmestad et. al., 2000*).

Water depth in the area is about 35 m.

The water area of the northeastern Sakhalin-I is influenced by cold currents and characterized by the annual average temperature of 2-3°C.

In the period of summer monsoon (June – August), prevailing wave direction is southeastern and southern, according to the observations. When winter monsoon season starts, repeatability of waves of northeastern and northern directions increases.

The only type of ice observed in the Sea of Okhotsk is first-year ice. The sea is covered with ice for 180 – 190 days on average.

Additional risks for the field development are caused by earthquakes occurring quite often in earthquake-prone region of Kurile Islands (*Gudmestad et al., 2000*).

Table 19: General information for the Southern Sea of Okhotsk – off Northeastern Sakhalin-Island Coast (*ISO 19906, 2010*)

Parameter	Value
Winter Season	7 months
Summer Season	5 months
Average minimum air temperature, °C	-36 to -44
10 minute average wind speed, m/s	24 to 34
Significant wave height (< 100 m water depth), m	9.5 to 14.0
Near surface maximum speed of current, cm/sec	139 to 338
Average water surface salinity, ppt	31.7 to 32.6
Summer average surface water temperature, °C	+10.4 to +11.5
Winter average water temperature, °C	-1.8 to 0
Seismic magnitude	7.0 to 7.5
Average ice-free period, days	155
First ice occurrence	25 October to 10 November
Last ice occurrence	20 May to 25 June
Level ice (first-year) thickness, m	0.7 to 1.21
Rafted ice thickness, m	2.0 to 3.3
Rubble fields sail height, m	4.4 to 6.0
Rubble fields length, m	80 to 160
Ridges sail height, m	5.4 to 8.1
Ridges keel depth, m	19.8 to 23.2
Stamukhi, m	< 26

According to Exxon Neftegas Limited, the operator of the Sakhalin-I Project, Arkutun-Dagi oil and gas field is characterized by the following features:

- Estimated recoverable reserves: 114.6 million tons of oil, 54.6 billion cubic meters of gas;
- Planned annual rate of oil production is ca. 4.5 million tons;
- The project life cycle will last until 2040 – 2050;
- 45 slots for deviated wells are designed (*Exxon Neftegas Limited, 2016*).

The field is developed by using the offshore platform “Berkut” weighting more than 200 thousand tons. It is located 25 km from the shore at water depth of 35 m. The production started in January 2015 (*Neftegaz.RU webpage, n.d.*).

The platform is capable to resist the loads of 18 m high waves and 2 m thick ice as well as extremely low temperatures down to -44°C and earthquakes with 9.0 magnitude on Richter scale.

The Berkut platform consists of two main parts:

- Ice-resistant gravity base structure (GBS) weighting ac. 160 thousand tons;
- Topside with integrated technological, drilling and living modules and other facilities.

The GBS is a rectangular-shaped concrete caisson, on which 4 concrete columns are installed to support the topside:

- Caisson length is more than 133 m;
- Caisson width is 100 m;
- Total height (caisson + columns) is about 55 m.



Figure 19: Offshore platform "Berkut" (Exxon Neftegas Limited, 2016)

The platform is equipped with fully winterized drilling rig capable for drilling 7 km long-reach wells and performing challenging completion jobs.

Production fluid is transported to the Chayvo onshore processing facility by subsea flowline. The hydrocarbons from Arkutun-Dagi field are pumped to the processing facility and then by main pipeline to the De-Kastri oil export terminal (Khabarovsk Krai) for further shipment (*Exxon Neftegas Limited, 2014*).

4.2. Newfoundland and Labrador Continental Shelf

Environmental conditions of Newfoundland and Labrador continental shelf can be described as harsh much like the northern North Sea. The minimum registered air temperature is -17.3°C . Maximum 100-year storm wave height is 27.4 m and the significant wave height is 14.7 m. The field development activities in the region are complicated by:

- a) “Large” icebergs (up to 6 million tons) “digging” the seafloor down to a depth of 1.5 m;
- b) Icing of the oil and gas facilities and floaters due to waves, wind and low temperatures;
- c) Intense storms occurring in winter season;
- d) Very restricted visibility due to fog, especially in July (*Husky Oil Operations Ltd., 2001*).

Table 20: General information for the Newfoundland offshore (*ISO 19906, 2010*)

Parameter	Value
Winter Season	December to April
Summer Season	May to November
Average minimum air temperature, $^{\circ}\text{C}$	-15 to -19
Freezing degree days	250 to 750
10 minute average wind speed, m/s	24 to 38
Significant wave height (> 100 m water depth), m	7.4 to 15.6
Near surface maximum speed of current, cm/sec	90 to 130
Summer average water temperature, $^{\circ}\text{C}$	+15 to +19
Winter average water temperature, $^{\circ}\text{C}$	-0.9 to +4.3
Average ice-free period, days	150
First ice occurrence	December to January
Last ice occurrence	May to June
Level ice (first-year) thickness, m	0.7 to 1.2
Rafted ice thickness, m	2.0
Rubble fields sail height, m	1.1
Rubble fields length, m	ND
Ridges sail height, m	4.5
Ridges keel depth, m	5.0
Iceberg mass, million tones	0.05 to 6.00
Presence of icebergs	All year round
Number of icebergs per year	0 to 2200
Ice induced gouge depth, m	0.1 to 1.5

4.2.1. “Hibernia” Project

Hibernia oil and gas field is located in the Jeanne d’Arc Basin, 315 km east of Newfoundland and Labrador in Canada. Average water depth is 80 m. The field was first discovered in 1979. Production started in November 1997.

The project is operated by Hibernia Management and Development Company Ltd. (HMDC). The ownership is shared between ExxonMobil Canada (33.125%), Chevron Canada Resources (26.875%), Suncor (20%), Canada Hibernia Holding Corporation (8.5%), Murphy Oil (6.5%) and Statoil Canada Ltd. (5%) (*Hibernia webpage, n.d.*).

According to the estimates of Canada – Newfoundland & Labrador Offshore Petroleum Board (C-NLOPB), proven recoverable resources of Hibernia field are:

- 1278 MMbbls of oil;
- 1764 Bscf of gas.

Cumulative oil production (as of December 31, 2017) is 973 MMbbls. Current average rate of extraction is 144,089 bbls / day. (*C-NLOPB webpage, n.d.*).

Hibernia field is developed using a special gravity base structure (GBS) manufactured in such a way to provide safety and reliability in the harsh conditions of the Grand Banks region. It is the first GBS in the world capable to withstand collision with an iceberg weighting more than 1 million tons (expected to occur once every 500 years) without damage to the environment and technological process (*Offshore Technology journal webpage, n.d.*).



Figure 20: Offshore platform “Hibernia” (*Hibernia official webpage, n.d.*)

Structurally, Hibernia platform consists of the three main systems: Gravity Base Structure, Topsides and Offshore Loading System (OLS) (*Hibernia official webpage, n.d.*).

The platform stands 224 m high. Hibernia's 450 thousand tons GBS (111 m high) was constructed using high-strength concrete reinforced with steel rods and pre-stressed tendons that create additional strength. The structure is equipped with serrated outer edges designed to counter icebergs. There are oil tanks inside the GBS, designed capacity of which is 1.3 million barrels of crude. Drilling operations are carried out via two drill shafts housing 32 drill slots each (*Offshore Technology journal webpage, n.d.*).

The topside is composed of the five super modules: wellhead, mud system, processing equipment, utilities and living quarters.

The Offshore Loading System provides the means to export oil stored in the tanks. The product is pumped out of the tanks via subsea pipelines and buoy to flexible loading hoses fabricated to feed specially designed shuttle tankers.

Additional infrastructure is built to support the production. It includes shorebase facilities, heliport and transshipment terminal (*Hibernia official webpage, n.d.*).

4.2.2. "Hebron" Project

Hebron oilfield is located ca. 32 km southeast of Hibernia platform. The water depth in the area is about 93 m. The field was discovered in 1980 and is estimated to produce more than 700 MMbbls of oil with peak rate of extraction up to 150 thousand barrels per day.

The project's operator is Exxon Mobil Canada Properties (35.5% of assets). Its co-owners are Chevron Canada Ltd. (29.6%), Suncor Energy Inc. (21%), Statoil Canada Ltd. (9%) and Nalcor Energy - Oil and Gas Inc. (4.9%).

Hebron oilfield is being developed using a stand-alone GBS fabricated of reinforced concrete capable to withstand icebergs, sea ice and challenging meteorological and environmental conditions. The structure is equipped with tanks designed to store about 1.2 million barrels of crude. Additionally, it serves as a support for integrated topsides accommodating drilling, production and processing facilities and living quarters (*Hebron Project official webpage, n.d.*).

According to the project, the hydrocarbons processed at Hebron platform are pumped out from the storage capacities to shuttle tankers using Offshore Loading System (OLS) that includes two pipeline segments routed from the GBS to subsea loading stations consisting of anchoring, valve and hose systems (*Hebron Project EOI, 2012*).

Table 21: The platform key metrics (*Hebron Project official webpage, n.d.*)

Parameter	Value
<i>GBS</i>	
Height, m	122
Diameter of base, m	130
Well slots	52
<i>Topside</i>	
Height, m	113
Operating weight, tones	65000
Accommodations (POB)	220
<i>OLS</i>	
Total crude handling capacity, m ³ /hr	5400
Pipelines length, m	6000
Number of loading stations	2



Figure 21: Hebron platform being towed-out to the field (*Hebron Project official webpage, n.d.*)

In November 2017, the first oil was produced from Hebron oilfield. It is noteworthy that the project has been put into operation ahead of schedule (*Hebron Project official webpage, n.d.*).

4.2.3. “White Rose” Project

The White Rose field is also located in the Jeanne d’Arc Basin, approximately 350 km off the east coast of Newfoundland and Labrador, Canada. Ownership of the project is shared between Husky Energy Inc. (72.5%) and Suncor Energy Inc. (27.5%). Discovered in 1984, the field is classified by the operating

company as a significant discovery area consisting of both oil and gas pools. The production started in 2005. Water depth in the area is approximately 120 m (*Husky Energy Ltd., 2012*).

The C-NLOPB estimated recoverable oil reserves at the field to be 404 MMbbls. According to the report on cumulative production, 232.2 MMbbls of oil and 6.78 BCM of gas have been recovered from the field. In 2016 – 2017, the daily average production was estimated at a level of ca. 30600 bbls/d (*C-NLOPB webpage, n.d.*).

The initial field development concept includes production from subsea wells in the excavated subsea drill centers (glory holes) to the SeaRose FPSO unit (floating production, storage and offloading) through flexible risers and flowlines. There are three drill centers originally:

- The Central Drill Center (CDC) and the Southern Drill Center (SDC);
- The Northern Drill Centre (NDC) that is used to inject gas stored for the future consumption (*Husky Oil Operations Ltd., 2001*).

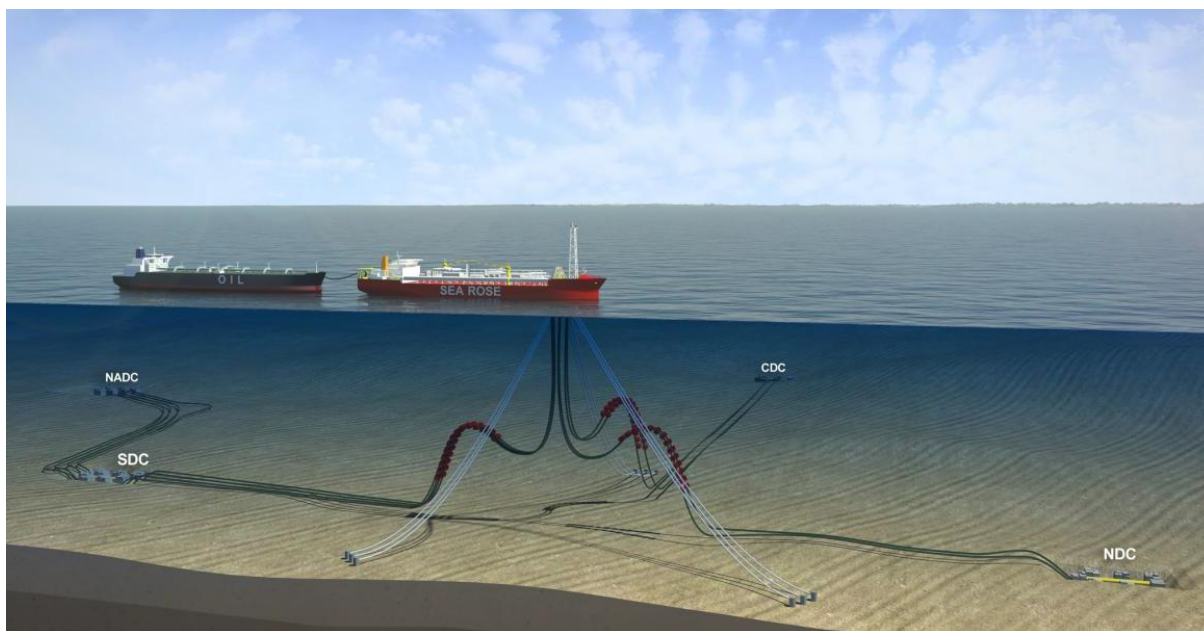


Figure 22: Field development concept of the White Rose field (Husky Energy Ltd., 2012)

The subsea field includes 42 km of flowlines, flexible risers and umbilicals, 21 Xmas trees and 5 manifolds as well as wellhead facilities, sea bottom structures, control, maintenance and inspection equipment (*Husky Oil Operations Ltd., 2001*).

Glory hole is an excavation into the seabed created to protect subsea facilities against powerful sea currents and icebergs scoring the ocean floor. In order to avoid contact with an iceberg keel, the top of wellhead equipment, Xmas trees and manifolds should have a minimum clearance of 2-3 m below the seabed level (approximately 9 m below the original surrounding seabed). This is due to the measured scour depths in the area of 1.5 m. The excavation was performed by

using trailing suction hopper dredger equipped with a deep dredging suction pipe (*Van Es et. al., 2004*).

As one more protection mean, weak link technology in flowlines and umbilicals was implemented in the project. The hazard of oil spill due to a flowline broken by iceberg scouring the seabed was mitigated by using this technology. Once the link is disconnected, the flowline is depressurized and circulated to water (*Norman et. al., 2008*).

After passing subsea wells the produced reservoir fluid is pumped up via flexible risers to turret of the Sea Rose FPSO and then to the process plant. Oil is stored in the FPSO tanks and then offloaded to shuttle tankers (*Husky Oil Operations Ltd., 2001*).

The Sea Rose is 258 m in length, 46 m in width and 18 m in height. The light-ship displacement of the vessel is ca. 31500 t. It carries the process facilities with 7400 t dry weight.

As the vessel is subject to ice loading during a winter period it was manufactured in ice-resistant design. In order to avoid iceberg threat, the FPSO is able to safely and promptly disconnect flexible risers and turret mooring lines and leave the location. In addition, the turret design enables the vessel to orient the bow towards the prevailing direction of the environmental loads (wind, waves and ice) (*Norman et. al., 2008*).

It is worth noting that the original field development concept of the White Rose project is still being supplemented by the extensions suggesting a number of the tie-ins to the main field (*Husky Energy Ltd., 2012*).

4.3. Cook Inlet and the Beaufort Sea

4.3.1. Offshore field development in Cook Inlet

Offshore field development in the Arctic and sub-Arctic continental shelf was initiated in the USA and Canada in 1960s. It was Cook Inlet where the first experience in oil and gas production activities challenged by severe ice conditions was gained (*Popp, 2006*).

Divided into three regions (Head, Upper and Lower), Cook Inlet represents 350 km long estuary on the Alaska southern coast. Depending on the particular region, water depths within the Inlet vary considerably:

- Shallow tidal regions in the Head region;
- Less than 70 m water depth in the Upper region;
- Less than 150 m water depth in the Lower region.

Due to the presence of ocean waters climate of Cook Inlet is characterized as maritime. In comparison with inland Alaska, winter air temperatures in the region are normally warmer and summer air temperatures are cooler.

Wind speed is relatively constant throughout a year. Coastal areas of Cook Inlet are subject to strong topographically-enhanced winds in winter season.

Fast currents and high tidal range are the key environmental features of the region. Tidal magnitude in the Inlet is one of the highest in the world. It varies throughout the region, with a mean value of 3.47 in the south to a mean value of 7.9 m in the north.

Cook Inlet is subject to seasonal ice cover, which appears in October. The largest ice fields normally form by late February-early March, while by mid-April all ice has melted. Generally, the ice environment can be characterized as very dynamic due to powerful tides and currents. The prevailing direction of ice drift is from north to south. Under action of tides, Cook Inlet ice forms rubble fields and stamukhi posing an additional hazard on the offshore structures (*ISO 19906, 2010*).

The main environmental features of the area are listed in the table below.

Table 22: General information for the Cook Inlet (*ISO 19906, 2010*)

Parameter	Value
Winter Season	October to April
Summer Season	May to September
Average minimum air temperature, °C	-20
Absolute minimum air temperature, °C	-43
10 minute average wind speed, m/s	20 to 32
Maximum significant wave height, m	4 to 5.5
Maximum tide and circulation, m/s	0 to 4
Average water surface salinity, ppt	10 to 30
Summer average surface water temperature, °C	+12 to +16
Winter average water temperature, °C	-2 to 0
Average ice-free period, days	230
First ice occurrence	17 October to 17 December
Last ice occurrence	10 March to 15 May
Level ice (first-year) thickness, m	0.6 to 0.9
Rafted ice thickness, m	1.2 to 1.5
Rubble fields sail height, m	0.5 to 2
Rubble fields length, m	100
Ridges sail height, m	1 to 2
Ridges keel depth, m	4 to 10
Stamukhi, m	4 to 12

According to the United States Geological Survey, undiscovered technically recoverable oil and gas reserves, both conventional and unconventional, in Cook Inlet are:

- 600 MMbbl of oil;
- 19 TCF of natural gas;
- 46 MMbbl of natural gas liquids (*USGS webpage, n.d.*).

For almost half a century, 16 stationary ice-resistant platforms were installed in Cook Inlet at water depths from 20 m to 50 m:

- 13 platforms of 4-leg pile-fixed type;
- 2 platforms of 3-leg pile-fixed type;
- 1 monopod platform.

All these offshore platforms are equipped with relatively thin supports in order to pass approaching ice fields cutting its edges. This design solution provides sufficient level of the resistance. It is worth noting, that Gulf of Mexico experience in the offshore structures fabrication was used as a basis when designing the platforms for Cook Inlet hydrocarbon resources development. However, those technical solutions were adopted for the harsh environmental conditions of Alaska. In particular, tubular supports were modified by increasing its diameter to protect the wells from direct collision with ice sheet. In addition, there are special protective shrouds installed on the supports in a waterline zone. A significant disadvantage of these platforms design is that vibrations of high magnitude occur during ice drift season (*Belmar Engineering, 2009*).

Dolly Varden (see the figure below) is a good example of 4-leg ice resistant platform. The legs having a diameter of ca. 5 m each are interconnected by bracings and horizontal tubular connections below the area affected by ice loading. The platform is fixed on the seabed by piles penetrated through the legs into the soil to a depth of 50 m. Annular space in the legs is filled with concrete for providing additional stability of the platform.

The development plan included drilling 35 wells via 3 legs: 22 oil wells, 2 gas wells and 11 waterflood injectors. The topside is equipped with storage tanks for waste oil, waste water and diesel. The design life is 20 years (*Belmar Engineering, 2009*).

Spurr platform is an example of 3-leg platform for Cook Inlet. It was manufactured in Japan and installed in the Trading Bay at water depth of 20 m in 1968. The legs diameter is about 4 m each. Six piles per leg were penetrated into the seabed at a depth of more than 50 m.



Figure 23: Offshore platforms of three possible configurations in Cook Inlet (Dolly Varden platform, Spurr platform, Monopod platform)

According to the project, 6 oil wells, 1 gas well and 2 water injection wells were completed in each leg through piling (*Belmar Engineering, 2009*).

Also, there is experience in operating a platform of “Monopod” type with a single support in Cook Inlet. It is installed at water depth of 22 m and able to resist 1.8 m thick ice loading. The leg (outer diameter is 8.7 m) is equipped with a lattice structure in its base. This structure consists of pipes and 2 slender pontoons, which can be used either for providing buoyancy when the structure is towed or as storage capacities in the operation mode. It is fixed on the bottom using 32 tubular piles (910 mm diameter each) penetrated into the seabed at a depth of 30 m.

The leg is 38 m high and has 18 drilling slots placed in the annular space between 2 cylinders the structure consists of. The topside has overall dimensions of 33.5 x 33.5 m and stands 18.2 m high above the sea level. The liquid ballast represented by oil-water mixture in pontoons and piles penetrated into the seabed provide the platform stability against possible environmental impacts. (*Belmar Engineering, 2009*).

4.3.2. “Molikpaq” Platform

Currently, there is relatively high commercial interest in hydrocarbon resources exploration and its possible development in the Beaufort Sea.

The Beaufort Sea is referred as a marginal sea of the Arctic Ocean and characterized by very harsh environmental conditions. According to the Canadian Ice Service (CIS) measurements recorded in Tuktoyaktuk, summer temperatures typically reach +15°C and winter temperatures drop to -40°C on average. Due to strong winds and low air temperatures, extreme wind chill occurs in the region.

The winds are basically influenced by dramatic temperature difference between the mainland and water. The prevailing wind direction ranges from the northeast to southeast (*Timco et. al., 2009*).

The flow in the ocean surface layers are mostly determined by the Beaufort Gyre circulating clockwise. The flow speed ranges from 5 cm/s to 10 cm/s and can be about 100 cm/s during storms.

Three main regions are distinguished in the sea depending on the ice types:

1) Polar pack zone, which is comprised of permanently present and continuously migrating multi-year ice (4.5 - 5.5 m thick) and ice ridges (up to 25 m thick).

2) Seasonal transitional zone primarily comprising of highly dynamic first-year ice as well as a great number of multi-year ice floes.

3) Landfast ice zone primarily comprising of first-year ice that ice reaches a maximum thickness of about 1.9 m.

There are several factors imposing additional challenges and risks on field development activities in the region:

1) Permafrost that can be several hundred meters thick and is deposited at a depth from 50 m to 150 m beneath the seafloor.

2) Shallow gas pockets and gas hydrate formations.

3) Large ice ridges migrating throughout the Beaufort Sea and heavily gouging the seabed down to a depth of 5 m (*ISO 19906, 2010*).

The main environmental features of the sea are listed in the table below.

Table 23: General information for the Beaufort Sea (*ISO 19906, 2010*)

Parameter	Value
Winter Season	October to July
Summer Season	August to September
Average minimum air temperature, °C	-20 to -40
10 minute average wind speed, m/s	18 to 32
Maximum significant wave height, m	1.8 to 8.5
Average water surface salinity, ppt	0 to 33
Summer average surface water temperature, °C	0 to +10
Winter average water temperature, °C	-2 to 0
Seismic magnitude	5.5. to 6.5
First ice occurrence	late-Sept to late-Oct
Last ice occurrence	early-July to mid-August
Level ice (first-year) thickness, m	1.5 to 2.3
Level ice (second and multi-year) thickness, m	2 to 11
Rafted ice thickness, m	2.5 to 4.5

Rubble fields (first-year) sail height, m	3 to 6
Rubble fields (first-year) length, m	100 to 1000
Rubble fields (second and multi-year) sail height, m	3 to 6
Rubble fields (second and multi-year) length, m	50 to 2300
Ridges (first-year) sail height, m	3 to 6
Ridges (first-year) keel depth, m	15 to 28
Ridges (second and multi-year) sail height, m	Significant
Ridges (second and multi-year) keel depth, m	10 to 35
Stamukhi, m	up to 20
Iceberg average mass, tons	10 million
Icebergs number per year	Poorly known
Seabed ice induced gouge depth, m	0.1 to 5

Experience in the Beaufort Sea field development characterized by harsh ice conditions demonstrated success of caisson structures application. The Molikpaq platform is an example of such facilities. The platform is referred to a Mobile Arctic Caisson (MAC) type. It was first used for exploratory drilling in the Canadian Beaufort Sea in 1984 (*Timco et. al., 2009*).

The Molikpaq was deployed for 4 winter seasons in the Canadian Arctic. It has a steel caisson with a continuous annulus of dimensions comparable with the platform dimensions. The inner space is filled with packed sand. This so-called “sand core” sitting on the seabed provides horizontal resistance of the facility.



Figure 24: Exploratory drilling rig “Molikpaq” in the Beaufort Sea (*Timco et. al., 2009*)

The Molikpaq outer face is designed in such a way to withstand extreme loads of large ice features. The structure can operate without a berm in water depths ranging from 9 to 21 m. In greater water depths, the structure is designed to sit on a submerged berm which can vary in depth, as required. Ballasting is entirely by water. To achieve the design resistance under dynamic load, densification of the hydraulically-placed core was required (*Timco et. al., 2009*).

According to the platform performance indicators, one can conclude that it is designed for year-round operation in the severe Arctic conditions at relatively shallow water depths.

The Molikpaq was purchased by Marathon Oil. It has been modified and is now being operated within “Sakhalin-II” project in Russia.

4.4. Intermediate results and recommendations for further studies

In this chapter, a detailed analysis of the various Arctic offshore oil and gas projects and regions where are implemented, has been carried out.

For searching the best technical and technological solutions in terms of their applicability to the North Wrangel area conditions, the following characteristics can be taken as the main ones:

- Water depth in a field;
- Remoteness of a field from shore;
- Volume of hydrocarbon reserves;
- Means of facilities protection from environmental impacts (ice, waves, low temperatures, etc.);
- Placement of development facilities’ main modules;
- Means of transporting produced fluid;
- Economic considerations.

The further study is recommended to focus on developing the criteria (including aggregated parameters), which would cover all the key environmental parameters in terms of their criticality and represent a ground for comparing the suggested analogues and selecting the most optimal conceptual solution for the North Wrangel license area.

Table 24: Cumulative information on environmental conditions in the considered regions

Parameter	Value					
	North Wrangel license area	Pechora Sea	Northeastern Sakhalin Coast	Newfoundland Offshore	Cook Inlet	Beaufort Sea
Winter Season	Oct - Jun	Oct to Jul	7 months	Dec to Apr	Oct to Apr	Oct to Jul
Summer Season	Jul - Sep	Aug to Sep	5 months	May to Nov	May to Sep	Aug to Sep
Winter min air temperature, °C	-40 to -51	-48	- 36 to -44	-15 to -19	-20 to -43	-20 to -40
10 minute max wind speed, m/s	30 to 34	20 to 25	24 to 34	24 to 38	20 to 32	18 to 32
Significant wave height, m	6 to 10	1.5 to 7.0	9.5 to 14.0	7.4 to 15.6	4 to 5.5	1.8 to 8.5
Near surface maximum speed of current, cm/s	70	100 to 130	139 to 338	90 to 130	0 to 400 (tide, circulation)	20 to 100
Average water surface salinity, ppt	25 to 29.5	25 to 33	31.7 to 32.6	31 to 33	10 to 30	0 to 33
Winter min water temperature, °C	-1.9 to 0	-1.8 to 0	-1.4 to 0	-0.9 to +4.3	-0.5 to +1.5	-2 to 0
Seismic magnitude	-	-	7.0 to 7.5	-	-	5.5 to 6.5
Ice-free period, days	0 to 74	110	155	150	230	60
First ice occurrence	Sept - Oct	Oct - Nov	Oct - Nov	Dec - Jan	Oct - Dec	Sept - Oct
Last ice occurrence	Jul - Aug	Jun - Jul	May - Jun	May - Jun	Mar - May	Jul - Aug
Level ice (first-year) thickness, m	1.5 to 1.9	0.7 to 1.1	0.7 to 1.21	0.7 to 1.2	0.6 to 0.9	1.5 to 2.3
Rafted ice thickness, m	No data	08. to 1.0	2.0 to 3.3	2	1.2 to 1.5	2.5 to 4.5
Rubble fields sail height, m	No data	No data	4.4 to 6.0	1.1	0.5 to 2.0	3 to 6
Rubble fields length, m	No data	No data	80 to 160	No data	100	100 to 1000
Ridges sail height, m	No data	3 to 4	5.4 to 8.1	4.5	1 to 2	3 to 6
Ridges keel depth, m	No data	15 to 18	19.8 to 23.2	5	4 to 10	15 to 28
Stamukhi, m	< 30	< 20	<26	No data	4 to 12	<20
Icebergs mass, million tons	No data	-	-	0.05 to 6.00	-	10
Number of icebergs per year	Sometimes	-	-	0 to 2200	-	Rare
Ice induced gouge depth, m	No data	No data	No data	0.1 to 1.5	No data	0.1 to 5.0

5. Possible development concepts study

The main purpose of this chapter is to identify the most efficient concept(s) in terms of:

- its ability to provide necessary production volumes (plateau production);
- economic effectiveness;
- reliability and flexibility to replace and repair equipment.

Since the study is being carried out in lack-of-data conditions, the Arctic best available practices described in the previous chapter shall be used as a basis for selecting the most appropriate development concept for the North Wrangel license area.

5.1. Development and ranking of criteria for comparison of the regions

The problem set for the conceptual studies of the North Wrangel license area at the initial stage, is the search for analogues by using aggregated parameters that characterize environmental conditions of the selected regions (not types of the development facilities). This is achievable by developing a list of criteria enabling the comparison of environmental conditions of the previously reviewed Arctic projects with each other and with the license area. In addition, these criteria should contribute to reasonable judgements on similarity / dissimilarity of these regions and feasibility of applying certain technological solutions for the field development.

The existing data array contains a sufficiently large number of parameters characterizing environmental conditions of the regions being compared. However, it should be noted that they do not fully describe the conditions, since they have been reduced in quantity for criticality to the structures' design basis considerations. Nevertheless, the fact of having even that number of parameters, as a rule, complicates the analysis, making it difficult for perception and subsequent research. In this connection, it is considered expedient to develop a simplified list consisting of the most significant comparison criteria, which in this case can be developed by:

- 1) highlighting and extracting the most critical parameters;
- 2) aggregating (grouping) several parameters to obtain the basic characteristics that affect selection of the concept.

First, it is necessary to designate parameters belonging to the first category. Undoubtedly, the following should be attributed to such parameters:

- water depth in the area of the field, which directly affects the type of development facilities;
- the distance from the drilling site to shore / supply bases / existing infrastructure, which affects the transportation of personnel and cargo, maritime logistics, a way of exporting hydrocarbons to the markets, etc .;
- seismicity of the region, which imposes additional technological difficulties and, as a consequence, requirements at the stage of designing offshore structures.

Next, aggregated criteria should be developed with justification of the chosen approach to classification of basic parameters.

Three main fields can be distinguished in the theory of classification:

- cluster analysis (clustering) and grouping;
- statistical analysis;
- discriminant analysis (*Orlov, 2009*).

Due to the specifics of a problem statement (to develop aggregated parameters for comprehensive comparative analysis of environmental conditions of the Arctic and subarctic seas) the study will be focused on the methods of clustering and grouping, which have a purpose of classes / groups identification.

In cluster analysis, the problem is to identify a natural partition into classes without influence of a researcher subjectivism, as well as to detect groups of similar objects having a sharp difference with the other groups. When grouping, a partition into groups takes place regardless of the naturalness of the partition boundaries. In other words, a researcher still sets as a goal to identify groups of homogeneous objects, but the boundaries between neighboring groups are rather arbitrary, unnatural and largely depend on the subjectivism of a researcher (*Orlov, 2009*).

In the considered case, it is necessary to divide the environmental parameters into groups regardless of whether the partition boundaries are natural or not (*Kendall et.al., 1976*), thereby the use of grouping method is justified.

The array of environmental parameters, except those previously identified as the most critical ones, was transformed by the method of grouping into 3 classes of homogeneous objects, hereinafter referred to as aggregated comparison criteria:

- Climatic conditions;
- Hydrological conditions;
- Ice conditions.

These aggregated criteria are considered important in terms of their individual and joint influence on the nature of external loads acting on the field development infrastructure and establishing requirements for the design of structures. Ice actions are particularly critical for the system integrity, which is confirmed by the calculations in Chapter 3.

The schemes of aggregation are shown below.

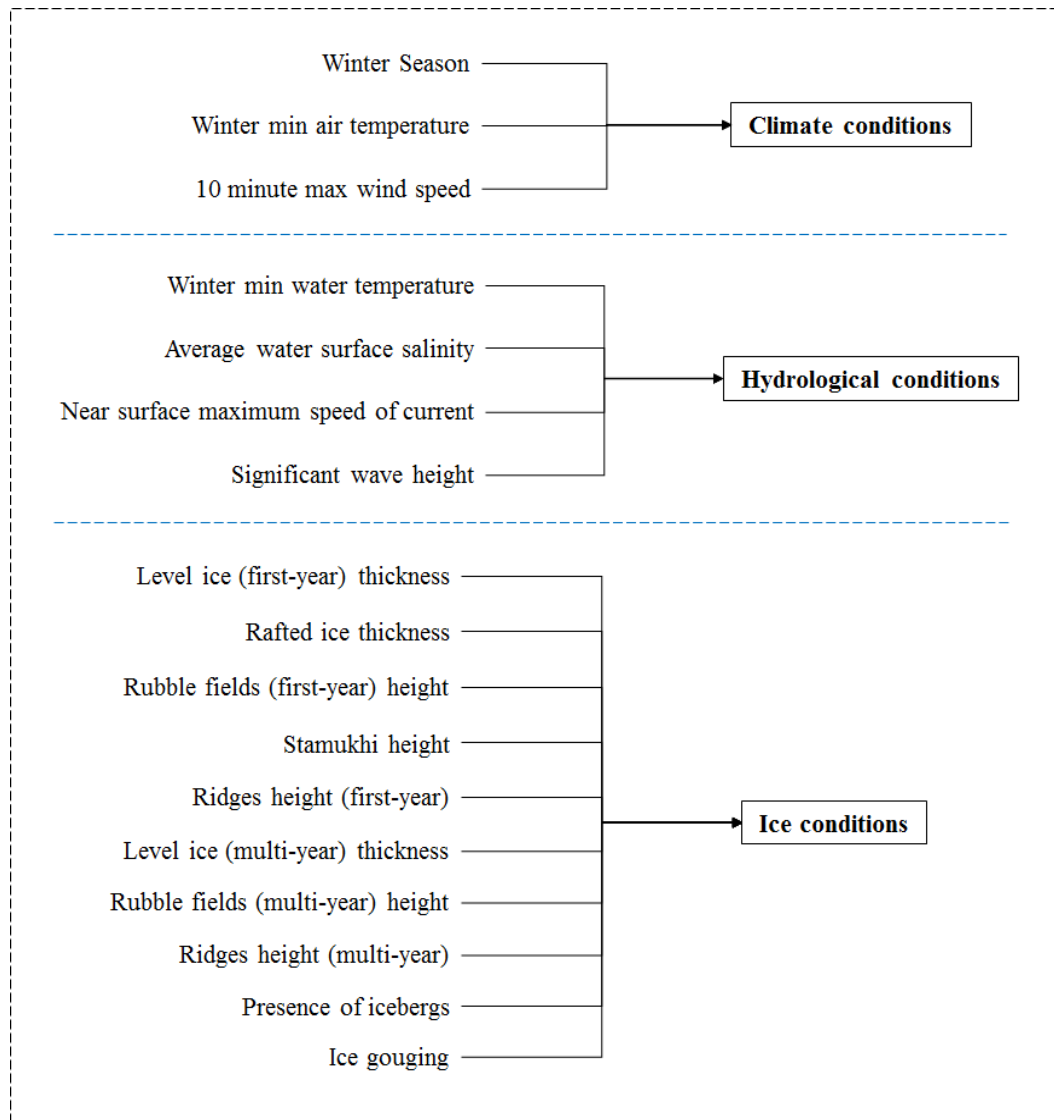


Figure 25: Aggregation (grouping) of the environmental parameters

Therefore, the following criteria were created to carry out a comparative analysis of different Arctic and sub-Arctic regions similar to the license area: water depth, distance to shore / supply bases / existing infrastructure, seismicity of the region, climate conditions, hydrological conditions, ice conditions.

Further, a question arises – how to competently compare the regions between each other using the indicated criteria? To answer it, let us refer to qualimetry, the science of measuring quality.

According to qualimetry, there are two main methods of measuring and assessing quality: instrumental and expert. The first is based on the use of indicators measured physically by special instruments (*Lisenkov et.al., 2009*). Obviously, in the study being held, water depth, distance to shore / supply bases and seismicity of a region are referred to this group, because these parameters are determined instrumentally. The second method supposes involvement of experts as a measuring tool. This method is widely used when it is physically difficult or impossible to determine qualitative characteristics (*Lisenkov et.al., 2009*). At first sight, this is valid for the aggregated criteria introduced since climate, hydrological and ice conditions cannot be evaluated unambiguously by means of a single tool only. However, this is not true because these criteria represent a set of other environmental parameters measured by physical methods each. It will be discussed in more detail further.

A comparative analysis of environmental conditions of the regions is much more convenient and expedient to carry out using different predetermined scales described by qualimetry approaches, e.g. a nominal scale or a ratio scale (*Lisenkov et.al., 2009*).

To solve the problem considered in this chapter, it is proposed to use a toolkit of so-called order scales allowing to rank the parameters as the intensity of their values increases. In other words, these scales enable to perform a gradation on the principle “more – less” (*Lisenkov et.al., 2009*). As a result of the analysis, a ranked range based on an expert evaluation is possible to show:

$$Q_1 > Q_2 > \dots > Q_n$$

In order to rationalize the analysis the reference points called ranks, shall be introduced and fixed in advance for further clear perception and proper application when comparing the parameters:

1	– Comfortable conditions
2	– Moderate conditions
3	– Intermediate conditions
4	– Complex conditions
5	– Harsh conditions

Depending on values of a certain environmental parameter, a corresponding rank will be assigned. It should be noted, that a rank is characterized not by a pointwise crisp value in the problem being solved but by a range of values (stochastic values). Such ranges and corresponding ranks are obtained expertly when comprehensively reviewing available environmental data of different Arctic seas. Maximum and minimum values are taken from a total range of values of a parameter, e.g. water depth or distance to shore. Then ranking is performed (assignment of ranks) by splitting a total range of values into intervals characterizing a particular rank. It is important to note that the ranking is also adjusted to the best practices and expert evaluation.

Thus, applying the described mechanism to criteria identified in the first part of this subchapter, we obtain the following ranks:

Table 25: Description of the comparison criteria ranks

Criteria	Ranks				
	1	2	3	4	5
Water depth, m	0 ÷ 25	25 ÷ 50	50 ÷ 75	75 ÷ 100	100 ÷ 125
Distance to shore / supply bases / existing infrastructure, km	0 ÷ 70	70 ÷ 140	140 ÷ 210	210 ÷ 280	280 ÷ 350
Seismicity, scores on the Richter scale	0 ÷ 1,6	1,6 ÷ 3,2	3,2 ÷ 4,8	4,8 ÷ 6,4	6,4 ÷ 8,0

As it can be seen, the rank of a particular region's characteristics is determined depending on its belonging to a certain interval. In case of the aggregated criteria, ranking is performed in a similar way. The difference here is that initially a rank is assigned to every environmental parameter that is a part of the criterion (a member parameter).

Table 26: Description of the aggregated comparison criteria ranks

Criteria	Member parameters	Ranks				
		1	2	3	4	5
Climate conditions	Winter season, days	120 ÷ 160	160 ÷ 195	195 ÷ 230	230 ÷ 265	265 ÷ 300
	Winter min air temperature, °C	-10 ÷ -20	-20 ÷ -30	-30 ÷ -40	-40 ÷ -50	-50 ÷ -60
	10 minute max wind speed, m/s	15 ÷ 20	20 ÷ 25	25 ÷ 30	30 ÷ 35	35 ÷ 40
Hydrological conditions	Winter min water temperature, °C	5,0 ÷ 3,6	3,6 ÷ 2,2	2,2 ÷ 0,8	0,8 ÷ -0,6	-0,6 ÷ -2
	Average water surface salinity, ppt	10 ÷ 15	15 ÷ 20	20 ÷ 25	25 ÷ 30	30 ÷ 35
	Near surface maximum speed of current, cm/s	0 ÷ 100	100 ÷ 200	200 ÷ 300	300 ÷ 400	400 ÷ 500
	Significant wave height, m	0 ÷ 3,2	3,2 ÷ 6,4	6,4 ÷ 9,6	9,6 ÷ 12,8	12,8 ÷ 16,0
Ice conditions	Level ice (first-year) thickness, m	0 ÷ 0,5	0,5 ÷ 1,0	1,0 ÷ 1,5	1,5 ÷ 2,0	2,0 ÷ 2,5
	Rafted ice thickness, m	0 ÷ 1	1 ÷ 2	2 ÷ 3	3 ÷ 4	4 ÷ 5
	Rubble fields (first-year) height, m	0 ÷ 1,6	1,6 ÷ 3,2	3,2 ÷ 4,8	4,8 ÷ 6,4	6,4 ÷ 8,0
	Stamukhi height, m	0 ÷ 6	6 ÷ 12	12 ÷ 18	18 ÷ 24	24 ÷ 30
	Ridges height (first-year), m	0 ÷ 7	7 ÷ 14	14 ÷ 21	21 ÷ 28	28 ÷ 35
	Level ice (multi-year) thickness, m	0	0	0 ÷ 4	4 ÷ 8	8 ÷ 12
	Rubble fields (multi-year) height, m	0	0	0 ÷ 2	2 ÷ 4	4 ÷ 6
	Ridges height (multi-year), m	0	0	0 ÷ 15	15 ÷ 30	30 ÷ 45
	Presence of icebergs	0	0	0	0	Yes
	Ice gouging	0	0	0	0	Yes

Further, to determine the aggregate rank, it is necessary to introduce a concept of the parameter's weight coefficient that characterizes its contribution to the criterion's rank.

One of the ways to determine the weight coefficients is expert evaluation using the Rosenberg scale. The method is based on a pairwise comparison of the member parameters in terms of their criticality for the integrity of structures and equipment. The comparison results are obtained taking into account the dominance of one parameter over another on the so-called Rosenberg scale that usually includes 4 levels of dominance (*Lisenkov et.al., 2009*).

Table 27: The Rosenberg scale

Level of dominance		Parameter 1	Parameter 2
1	Absolute dominance	6	0
2	Obvious dominance	5	1
3	Simple dominance	4	2
4	No dominance (equivalence of indicators)	3	3

The following results were obtained after the evaluation of parameters (we denote them by x_i) characterizing climate conditions and having a corresponding weight coefficient w_i given expertly in the last column of the table below (*Gazprom Neft Shelf, 2018*). In this case:

x_1 – winter season, days;

x_2 – winter min air temperature, $^{\circ}\text{C}$

x_3 – 10 minute max wind speed, m/s.

Table 28: The results of expert evaluation of the climatic parameters' weight coefficients, using the Rosenberg scale (*Lisenkov et.al., 2009*)

	x_1	x_2	x_3	Σ_i	$w_i = \frac{\Sigma_i}{\Sigma}$
x_1	3	2	5	10	$10/27 = 0,370$
x_2	4	3	5	12	$12/27 = 0,444$
x_3	1	1	3	5	$5/27 = 0,185$

$$\Sigma = 27$$

As can be seen from the table, the minimum air temperature in winter is the most significant member parameter of the aggregated criterion.

Further, it is necessary to expertly evaluate (*Gazprom Neft Shelf, 2018*) the remaining criteria using the Rosenberg scale. In the analysis of hydrological conditions, the following designations are assigned to the parameters:

- x_1 – winter min water temperature, °C;
- x_2 – average water surface salinity, ppt;
- x_3 – near surface maximum speed of current, cm/s;
- x_4 – significant wave height, m.

Table 29: The results of expert evaluation of the hydrological parameters' weight coefficients, using the Rosenberg scale (*Lisenkov et.al., 2009*)

	x_1	x_2	x_3	x_4	Σ_i	$w_i = \frac{\Sigma_i}{\Sigma}$
x_1	3	4	2	1	10	10/48 = 0,208
x_2	2	3	2	0	7	7/48 = 0,146
x_3	4	4	3	1	12	12/48 = 0,250
x_4	5	6	5	3	19	19/48 = 0,396
					$\Sigma = 48$	

The analysis clearly shows that a significant wave height makes the greatest contribution to the aggregated criterion characterizing hydrological conditions of the regions.

Using the same approach, we also should evaluate weight coefficients of parameters describing the ice conditions.

- x_1 – level ice (first-year) thickness, m;
- x_2 – rafted ice thickness, m;
- x_3 – rubble fields (first-year) height, m;
- x_4 – stamukhi height, m;
- x_5 – ridges height (first-year), m;
- x_6 – level ice (multi-year) thickness, m;
- x_7 – rubble fields (multi-year) height, m;
- x_8 – ridges height (multi-year), m;
- x_9 – presence of icebergs;

x_{10} – ice gouging.

Table 30: The results of expert evaluation of the ice parameters' weight coefficients, using the Rosenberg scale (*Lisenkov et.al., 2009*)

	x_1	x_2	x_3	x_4	x_5	x_6	x_7	x_8	x_9	x_{10}	Σ_i	$w_i = \frac{\Sigma_i}{\Sigma}$
x_1	3	2	3	1	1	2	2	0	0	0	14	$14/299 = 0,047$
x_2	4	3	4	2	1	3	3	0	0	0	20	$20/299 = 0,067$
x_3	3	2	3	1	1	2	1	0	0	0	13	$13/299 = 0,043$
x_4	5	4	5	3	2	4	4	1	0	2	30	$30/299 = 0,100$
x_5	5	5	5	4	3	4	4	2	1	2	35	$35/299 = 0,117$
x_6	4	3	4	2	2	3	3	1	1	1	24	$24/299 = 0,080$
x_7	4	3	4	2	2	3	3	1	1	1	24	$24/299 = 0,080$
x_8	6	6	6	5	4	5	5	3	2	2	44	$44/299 = 0,148$
x_9	6	6	6	6	5	5	5	4	3	4	50	$50/299 = 0,167$
x_{10}	6	6	6	4	4	5	5	4	2	3	45	$45/299 = 0,151$

$$\Sigma = 299$$

According to the table, the most significant parameters are presence of icebergs, ridges height (first-year and multi-year) and stamukhi height. Ice gouges formed due to contact of the ice keel with seafloor is a crucial factor as well. The other parameters are also important, but to a lesser extent, and will be taken into account when assigning an aggregate rank.

5.2. Comparative analysis of the regions

The next stage of the study is a comparative analysis of the conditions of the Arctic regions and the North Wrangel license area. Having values of the environmental parameters and the conditions for assigning them one or another rank, one can rank these data. On this basis, it is permissible to compare. Below is

a table with the ranking results for the first group of comparison criteria described in the previous subchapter.

Table 31: Ranking the criteria for comparing regions

	License area	Pechora Sea	Sakhalin Offshore	Grand Banks	Cook Inlet	Beaufort Sea
Water Depth	4	1	2	4	2	1
Distance to shore / supply bases / existing infrastructure	5	1	1	5	1	1
Seismicity	1	1	5	1	1	4

The ranking of aggregated criteria characterizing climatic, hydrological and ice conditions of the regions being compared is carried out in two stages. First of all, the ranks are assigned to the parameters included in the aggregated criteria, as shown in table 32. Next, we estimate aggregate ranks using weight coefficients of each of the environmental parameters according to the following relationship (see table 33):

$$R = \sum_{i=0}^n w_i \cdot r_i,$$

where: R – aggregate rank,

r_i – rank of a member parameter,

w_i – weight coefficient of a member parameter,

n – number of parameters aggregated into the criterion.

Table 32: Ranking the member parameters

Aggregated criteria	Member parameters	License area	Pechora Sea	Sakhalin Offshore	Grand Banks	Cook Inlet	Beaufort Sea		
Climate conditions	Winter season	5	5	3	1	2	5		
	Winter min air temperature	5	4	4	1	3	3		
	10 minute max wind speed	4	2	4	4	3	3		
Hydrological conditions	Winter min water temperature	5	5	4	1	3	5		
	Average water surface salinity	4	4	5	5	2	3		
	Near surface maximum speed of current	1	2	3	2	4	1		
	Significant wave height	3	2	5	5	2	2		
Ice conditions	Level ice (first-year) thickness	4	3	2	2	2	5		
	Rafted ice thickness	ND	3	3	2	2	4		
	Rubble fields (first-year) height	ND	ND	3	1	1	4		
	Stamukhi height	5	4	4	1	2	4		
	Ridges height (first-year)	ND	4	4	2	2	5		
	Level ice (multi-year) thickness	3	1	1	1	1	5		
	Rubble fields (multi-year) height	ND	ND	1	1	1	5		
	Ridges height (multi-year)	ND	1	1	1	1	5		
	Presence of icebergs	5	1	1	5	1	5		
	Ice gouging	ND	1	1	5	1	5		
1	Comfortable conditions	2	Moderate conditions	3	Intermediate conditions	4	Complex conditions	5	Harsh conditions

Table 33: Ranking aggregated comparison criteria taking into account weights of member parameters

Member parameters	License area			Pechora Sea			Sakhalin Offshore			Grand Banks			Cook Inlet			Beaufort Sea		
	r_i	w_i	R	r_i	w_i	R	r_i	w_i	R	r_i	w_i	R	r_i	w_i	R	r_i	w_i	R
<i>Climate conditions</i>																		
Winter season	5	0.370	5	5	0.370	4	3	0.370	4	1	0.370	2	2	0.370	3	5	0.370	4
Winter min air temperature	5	0.444		4	0.444		4	0.444		1	0.444		3	0.444				
10 minute max wind speed	4	0.185		2	0.185		4	0.185		4	0.185		3	0.185				
<i>Hydrological conditions</i>																		
Winter min water temperature	5	0.208	3	5	0.208	3	4	0.208	4	1	0.208	3	3	0.208	3	5	0.208	3
Average water surface salinity	4	0.146		4	0.146		5	0.146		5	0.146		2	0.146				
Near surface maximum speed of current	1	0.250		2	0.250		3	0.250		2	0.250		4	0.250				
Significant wave height	3	0.396		2	0.396		5	0.396		5	0.396		2	0.396				
<i>Ice conditions</i>																		
Level ice (first-year) thickness	4	0.047	5	3	0.047	3	2	0.047	2	2	0.047	3	2	0.047	1	5	0.047	5
Stamukhi height	5	0.100		4	0.100		4	0.100		1	0.100		2	0.100				
Level ice (multi-year) thickness	4	0.080		1	0.080		1	0.080		1	0.080		1	0.080				
Presence of icebergs	5	0.167		1	0.167		1	0.167		5	0.167		1	0.167				

As the table 32 shows, not all parameters describing ice conditions were included in the analysis. This is due to the fact that currently ice conditions of the East Siberian Sea are still insufficiently explored, which in turn imposes certain limitations on the study. For the comparative analysis objectivity considerations, the aggregate ranks of the other regions were obtained using the same range of parameters as for the license area.

Reducing the number of parameters led to a revision of the expert assessment results and the weight coefficients assigned, which is reflected in the table below.

Table 34: The results of expert evaluation of the ice parameters' weight coefficients taking into account the lack of data

	x_1	x_4	x_6	x_9	Σ_i	$w_i = \frac{\Sigma_i}{\Sigma}$
x_1	3	1	2	0	6	$6/48 = 0,125$
x_4	5	3	4	2	14	$14/48 = 0,292$
x_6	4	2	3	1	10	$10/48 = 0,208$
x_9	6	4	5	3	18	$18/48 = 0,375$
	$\Sigma =$				48	

Table 35: Comparative analysis of environmental conditions of the license area and the regions

Criteria	License Area	Pechora Sea	Sea of Okhotsk	Grand Banks	Cook Inlet	Beaufort Sea
Water Depth	4	1	2	4	2	1
Distance to shore / supply bases / existing infrastructure	5	1	1	5	1	1
Seismicity	1	1	5	1	1	4
Climate	5	4	4	2	3	4
Hydrologic Conditions	3	3	4	3	3	3
Ice Conditions	5	3	2	3	1	5
1 Comfortable conditions	2 Moderate conditions	3 Intermediate conditions	4 Complex conditions	5 Harsh conditions		

Thus, the summary table has been developed. It demonstrates the degree of similarity / dissimilarity between the conditions of the North Wrangel license area and the regions selected for the analysis. It is well seen that there are no areas absolutely identical according to the selected criteria, but some intersections are observed everywhere. This indicates a certain degree of the similarity, which in turn means that the search for the best practices is carried out in the field where comparison of the regions is permissible and the judgments about the applicability / inapplicability of certain technical solutions are justified.

According to criteria “Water depth” and “Distance to shore / supply bases / existing infrastructure”, which are particularly crucial for a field development concept and its cost, the North Wrangel license area is similar to the Grand Banks, where “Hibernia”, “Hebron”, “White Rose” and “Terra Nova” projects are implemented.

The next parameter (seismicity) is characterized by comfortable conditions for the North Wrangel area. This means that there is no need for special design solutions to eliminate oscillations in case of using gravity platforms. In this regard, the license area is close to most of the reviewed projects.

Severe climate conditions are inherent in almost every region considered except of the Cook Inlet and the Grand Banks. This could be the basis for application of similar technical solutions for protection of the facilities, i.e. winterization.

Hydrological conditions are similar for all the regions considered except of the sub-Arctic region, where the Sakhalin projects are being implemented in particular.

Finally yet importantly, ice conditions being expertly evaluated criterion in accordance with the license area data available, are close enough to the Beaufort Sea conditions. This sea is also characterized by appearance of icebergs, multi-year ice and ice ridges. It is necessary to keep in mind that the ranking in this case could be done differently if sufficient data would be available. For instance, ice conditions of Newfoundland continental shelf are described in the literature (*ISO 19906, 2010*) as rather moderate except for the presence of icebergs. However, due to the fact only four parameters (including icebergs) were used in the evaluation of aggregated criterion, the region was given a rank of intermediate conditions. Such

nuances should be taken into account when selecting technological solutions for the field development in the license area.

5.3. Selection of the most feasible solution

Technical solutions used to develop oil and gas fields within the projects touched upon in this thesis are briefly described in the table below.

Table 36: The facilities used for the field development in the analyzed regions

Region	Facilities
Pechora Sea	Ice-Resistant Gravity Based Structure (IRGBS) Prirazlomnaya: drilling, production, processing, storage, offloading. The gravity based structure is equipped with sloping walls to take ice loads more efficiently (<i>Gazprom Neft Shelf, 2011</i>).
Sakhalin Offshore	Berkut platform: drilling, production. Onshore: processing, storage, offloading. The GBS is capable to resist earthquakes with 9.0 magnitude on Richter scale (<i>Exxon Neftegas Limited, 2014</i>).
Grand Banks	<ul style="list-style-type: none"> Hibernia platform: drilling, production, processing, storage, offloading via buoy. The world's first gravity platform capable to withstand a collision with an iceberg (<i>Hibernia, 2018</i>). Sea Rose FPSO: processing, storage, offloading. The vessel is equipped with emergency disconnection system. Production is carried out from subsea wells located in the glory holes and connected to the FPSO by flexible risers and flowlines (<i>Husky Energy Ltd., 2001</i>).
Cook Inlet	4-leg pile-fixed platforms (13), 3-leg pile-fixed platforms (2), 1 mono-leg pile-fixed platform. Hydrocarbons are transported to the shore through subsea pipeline. Ice-resistant thin supports equipped with protective shrouds are buried into sea bottom down to 50-70 m (<i>Belmar Engineering Services Ltd., 2009</i>).
Beaufort Sea	Molikpaq exploratory drilling rig: steel caisson with sand core. At water depths of more than 21 m, the use of bulk berm is designed (<i>Timco et.al., 2009</i>).

When analyzing various concepts of hydrocarbon resources development in the North Wrangel license area, it is necessary to limit the scope of potentially applicable solutions based on the results of the status of technologies study.

Since the technological approaches of all the described projects are in one way or another permissible for the license area, each of them will be considered initially:

- Concrete GBS;
- Pile-Fixed Platform (Jacket);
- Mono-Leg Fixed Platform (Monopod);
- FPSO (Ship Shaped Platform).

Further, based on the results of the applicability assessment, the most feasible concept(s) will be selected.

A matrix with a structured description of these conceptual solutions is given on the next page.

Systematization of information about environmental conditions of the license area (see Chapters 2, 4 of this work) allows us to outline the following main features:

- Water depths range from 20 m to 100 m;
- Distance from the from the southern border of the license area to the shore is about 140 km;
- Ice-free period is from 0 to 74 days;
- Appearance of icebergs is possible;
- Significant wave height is about 10 m;
- Average level ice thickness is more than 2 m;
- Maximum level ice thickness (1/100 yr.) is more than 3 m.

Taking into account the license area environmental features (extremely short ice-free period, large distance to the shore, presence of icebergs and multi-year ice fields of more than 2 m thick), well construction and production using pile-fixed steel platforms (monopod, jacket) are not possible (*Nikitin et.al., 1999*). Significant ice loads and large distance to the coast do not provide the possibility of installing the platform at the drilling site.

Table 37: Matrix of the conceptual solutions for the field development in the North Wrangel license area (INTECSEA Inc., 2012)

Facility Type	Major Capability			Water Depth, m	Ice Conditions		Design for Icebergs	Disconnectable	Tree Type		Location Appl.		Envir. Condit.		Risers			Export /Disposal Methods							
	Exploration	Production	Production Storage		One-year ice	Multi-year ice			Wet	Dry	Nearby Infrastructure	Remote	Calm	Significant Seas	Oil / Condensate			Gas							
															Steel Catenary Risers (SCR)	Flexible Risers	Internal Steel Risers	Oil Export Pipeline	Shuttle Tankers	Oil to Wire (convert to electricity)	Gas Export Pipeline	Liquefied Natural Gas	Compressed Natural Gas	Gas to Wire (convert to electricity)	Fuel Gas
Concrete GBS	Field Proven	Field Proven	Field Proven	up to 80-100	Field Proven	Field Proven	Field Proven	Does not meet requirements	Does not meet requirements	Field Proven	Field Proven	Field Proven	Field Proven	Field Proven	Field Proven	Field Proven	Field Proven	Field Proven	Field Proven	Field Proven	Field Proven	Field Proven	Field Proven	Field Proven	
Pile-Fixed Platform	Does not meet requirements	Field Proven	Does not meet requirements	up to 70	Field Proven	Does not meet requirements	Does not meet requirements	Does not meet requirements	Field Proven	Field Proven	Field Proven	Field Proven	Field Proven	Field Proven	Field Proven	Field Proven	Qualified	Concept	Field Proven	Concept	Concept	Field Proven	Qualified		
Mono-Leg Fixed Platform	Does not meet requirements	Field Proven	Does not meet requirements	up to 80	Field Proven	Does not meet requirements	Does not meet requirements	Does not meet requirements	Field Proven	Field Proven	Field Proven	Field Proven	Field Proven	Field Proven	Field Proven	Field Proven	Qualified	Concept	Field Proven	Concept	Concept	Field Proven	Qualified		
FPSO	Field Proven	Field Proven	Field Proven	Up to 100	Concept	Field Proven	Field Proven	Field Proven	Does not meet requirements	Field Proven	Field Proven	Field Proven	Field Proven	Field Proven	Field Proven	Field Proven	Field Proven	Field Proven	Field Proven	Field Proven	Field Proven	Field Proven	Field Proven		

Field Proven
 Qualified
 Concept
 Does not meet requirements
 Not Applicable

Exploratory drilling in such conditions is theoretically possible using ship-shaped platforms (drilling vessels) providing quick installation / take off from the drilling site, subject to obligatory ice management (*Nikitin et.al., 1999*). However, drilling season cannot be long enough in this case to enable constructing even a single exploration well. Drilling in the North Wrangel area is also complicated by probable supply problems due to the lack of coastal bases within a radius of hundreds of kilometers and a short navigational season.

To ensure year-round drilling and production under such conditions, it is advisable to consider ice-resistant concrete gravity based platforms. Due to buoyancy and availability of ballasting systems, this facility can be towed over long distances and installed in relatively short period without the use of expensive crane vessels and special barges. This is extremely important for a license area located at significant distances from main fabrication sites and characterized by a short ice-free period. In addition, the GBSs are usually autonomous and have excellent strength properties, providing resistance to external loads and minimum maintenance requirements. In terms of environmental friendliness, these platforms are equipped with reliable protection systems against pollution of water areas, which is very crucial in the Arctic region. When using this platform type, it is necessary to be aware of sea bottom soils properties affecting stability of a gravity based structure (*Nikitin et.al., 1999*).

Thus, ice-resistant gravity platform with concrete foundation is the best technical solution for oil and gas resources development in the North Wrangel license area. Based on this, several field development concepts can be generated.

5.4. Description of the most feasible field development concepts

After the analysis of the long list of the field development options, the shortened list consisting of three different concepts is presented in this subchapter (*Zolotukhin et.al., 2000*).

- *Concept I* – production platform(s) (drilling, production, processing, storage); direct offloading from the platform; oil transportation by Arctic class tankers.

- *Concept II* – production platform (drilling, production, processing, storage) + wellhead platform (drilling, production); direct offloading from the platform; oil transportation by Arctic class tankers.
- *Concept III* – subsea tieback to production platform; direct offloading from the platform; oil transportation by Arctic class tankers.

Due to the fact that currently there is no reliable information about expected traps outlines, estimated reserves in traps, reservoir depth, properties of hydrocarbons in-place, the proposed options are considered equally applicable. This corresponds to the goal that was set in this master's thesis – to prepare a comprehensive basis for possible development and arrangement scenario.

As it has already been noted, a massive production platform equipped with sufficiently powerful drilling equipment, processing plant, storage tanks and other facilities needed to maintain a field in production takes a central position in the study. At the same time, this concept can be modified according to the outlined arrangement options. There are a number of factors influencing the selection of a certain option.

1) Geological features

The geological structure largely determines how the field development will be implemented.

a) Depending on proven recoverable reserves, at the conceptual design stage a decision on number of platforms and the way they should be located is taken. In case of large forecasted production volumes, the use of one platform is inadvisable, since its weight and size may be too large. This will lead to unreasonable jump in the costs for manufacturing, towing, installation etc. To avoid this, it is customary to use two production platforms of smaller weight and size or one production platform and one wellhead platform. Wellhead platforms, as a rule, have a minimum number of systems and are installed as auxiliary production units (Zolotukhin et.al., 2000).

b) If it is not possible to drain the marginal zones by drilling directional wells from a production platform or a wellhead platform, the use of subsea production system can be considered. In addition, if the license area resources are developed as a cluster (along with large geological structures small satellite fields are developed), subsea production can be a feasible solution (*Nikitin et.al., 1999*).

However, in case of using these systems in the region being considered it is necessary to be aware of water depths at which subsea facilities are installed, and duration of ice-free period.

2) Water depth

Ice-resistant gravity platforms can be used in any geographical point of the North Wrangel license area, except of a narrow section on the northwestern edge, where a rather steep continental slope begins. This factor has a direct impact on the integrity of subsea pipelines and the range of subsea production systems applicability. For instance, in case of subsea field development on the southern border of the license area, there is a significant risk of the equipment damage with subsequent environmental consequences due to possibility of large ice ridges and icebergs appearance, which are able to gouge the seabed. The solution in this case is burial of subsea equipment and pipelines in seafloor.

In terms of capital expenditures, water depth is a very important parameter. With respect to gravity platforms, the following relationship is valid: smaller depth - smaller height of platform foundation - less use of materials for construction - less cost of a production platform.

3) Distance to the shore (Pevek seaport)



Figure 26: Dependence on distance to shore

Depending on distance from a production platform to the shore, the concepts can be modified by adding intermediate platform that is recommended to be installed at the southern corner of the license area to provide intermediate means for refueling helicopters as well as to perform auxiliary functions for rescue operations. The figure shows an arrangement concept without constructing an intermediate platform (blue arrow) and with having it installed (orange arrows).

5.4.1. Recommendations on the main structures and facilities for the field development of the North Wrangel license area

1) Platforms

The described arrangement concepts assume the use of ice-resistant gravity platforms different in major capabilities. This in turn is reflected on the design.

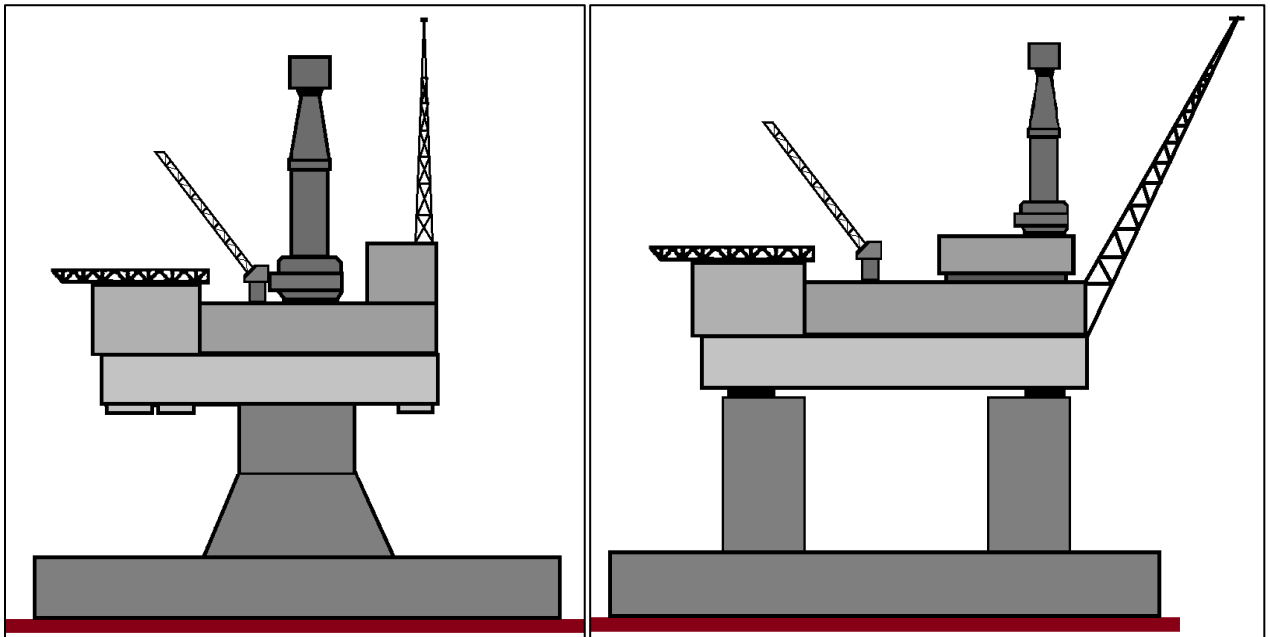


Figure 27: Schematic representation of possible configurations of the production platform

Topsides of the proposed configurations are identical consisting of modules for simultaneous drilling and operation of a cluster of wells. Both topsides include five main blocks: operational, drilling, energy, living quarters and life-support (Nikitin et.al., 1999).

The platform foundations are different fundamentally. Since ice conditions of the East Siberian Sea are extreme, it is the ice loads that will cause the greatest external impacts. Therefore, the structure must be selected in such a way as to ensure maximum reliability.

The first configuration (see Figure 29) is a massive, single-column, cone-shaped structure placed on a foundation block that has a cellular structure inside (*Nikitin et.al., 1999*). This configuration is stable enough to the ice fields' impacts (thick walls made of reinforced concrete), however its application is limited by the mass of topside.

A wellhead platform for the North Wrangel license area can also be manufactured in this way but more simplified.

As a rule, a greater number of supports increase the global effect of ice on the structure. In case of using the second proposed configuration for the production platform (see Figure 29), that is a four-column structure on a common foundation, there are two challenges arising:

- how to account for the mutual influence of supports;
- how does ice accumulated between the supports affect the global loads (*Nikitin et.al., 1999*).

The first challenge is solved by analyzing the appropriate graphs, which allow determining the load on a multi-leg structure as a whole, depending on the diameter of supports, the distance between them and the direction of ice movement.

The second one does not have an exact solution at the moment. Therefore, it is often assumed that the entire space between the columns is clogged with ice. The ice action in this case is determined as the load on an impenetrable barrier with dimensions corresponding to the outer line of the structure (*Zolotukhin et.al., 2000*).

At the same time, four-column structures provide sufficient stability of the platform in ice conditions as the extensive experience of its application in Sakhalin offshore shows. The outer wall of supports at waterline level can also be covered with clad steel to smooth the wave loads and improve the strength characteristics of the structure with respect to ice loads (*Neftegaz.RU webpage, n.d.*). Greater number of supports allows large mass of the topside as compared to the mono-column solution.

An intermediate platform used mainly as a base for refueling helicopters and as an auxiliary unit for rescue operations, is reasonable to manufacture using the

same design basis as for production platform. It should be the ice-resistant single-support GBS as shown in Figure 30.

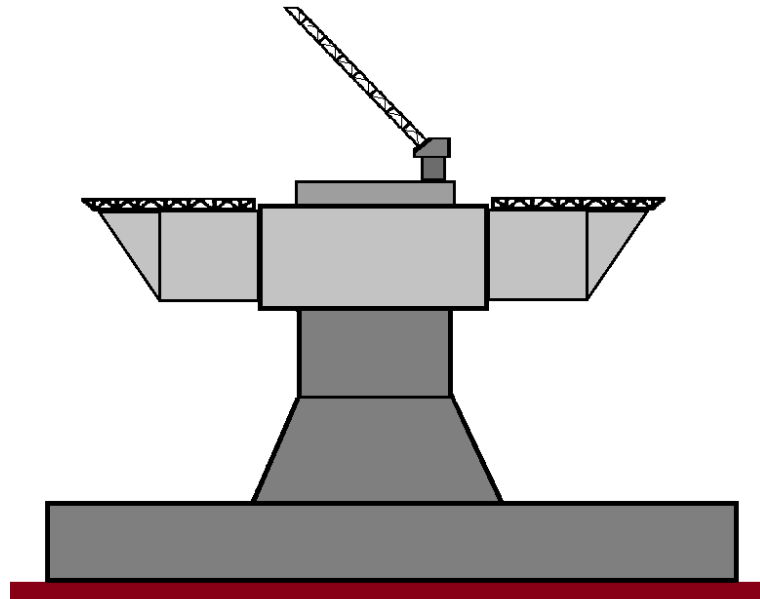


Figure 28: Schematic representation of the intermediate platform possible configuration

Due to the fact that the southern border of the license area, where the platform can be installed, is characterized by relatively mild ice conditions (compared to the northern part of the North Wrangel area), the requirements for the strength characteristics of this structure are supposed to be lower. In combination with a small water depth (20 m), this fact reduces the capital expenditures of the platform fabrication.

2) Subsea Production Systems

Due to large distances to the shore, subsea production systems are considered only in case of tieback to production platform. The systems can be introduced if it is not possible to drain the marginal zones by drilling directional wells or there are small satellite fields developed within cluster field development strategy.

As it has been already noted, in the shallow areas there is a possibility of gouging by large ice formations and icebergs, which imposes certain limits in the use of subsea facilities. To mitigate this, subsea and other technical systems installed on the seabed are buried in the soil so that the minimum clearance from the top points of the equipment is 1.5 - 2 m below the maximum gouge depth.



*Figure 29: Subsea equipment and pipeline burial in the sea bottom
(National Petroleum Council, 2015)*

The main obstacle in application of subsea production systems is extremely short ice-free period (0+ months) that limits the range of the drilling vessels use. This vessel can quickly anchor at the drilling site and leave the location if ice management is carried out. However, one drilling season will obviously not be enough to drill even a single well.

In 2013, Aker Solutions published the results of the drilling vessel model tests. According to the document, ice management allows reducing the global ice loads on the hull down to 50% (*Hannus, 2013*). The research held by JSC “Rubin” showed that ice management, which provides the conditions of brash one-year ice, allows reducing global ice actions by an order of magnitude (up to 10 times) compared to loads from level ice of similar thickness. Thus, ice management is a necessary condition for the expansion of drilling season in the license area.

5.4.2. Recommendations on oil transportation

Oil export from the North Wrangel license area is possible by two routes: Western (to Murmansk and further to European countries) and Eastern (to South Korea). Due to shorter distance and less severe climate and ice conditions, the Eastern route can be selected as a basic export option. Due to the milder environmental conditions and relative geographic proximity of importing countries in the eastern direction, the fleet of Arctic class tankers may be smaller in number compared to the western one. It is also obvious that the delivery time is significantly shorter in case of the selected option.



Figure 30: Concept of oil transportation by the Eastern route

According to the proposed concept, oil processed at the platform can be offloaded directly by the offloading facilities to Arctic class tankers (ARC 8) for further export to Asian countries, primarily to the Republic of Korea.



Figure 31: Direct oil offloading on the example of IRGBS Prirazlomnaya

It is also possible to install an intermediate floating terminal in the Anadyr Gulf (Bering Sea) area for reloading oil from Arctic class tankers to ordinary ones in order to optimize delivery schedules. Ordinary tankers in this case carry out delivery to the final consumer.

The transport logistic scheme of the project should also include icebreaker fleet and supply vessels for managing ice conditions during offloading, ensuring technological and environmental safety of works (*Gazprom Neft Shelf, 2013*).

6. CAPEX estimate for construction of the GBS

Due to the extremely low geological study of the license area, it is impossible to perform a reliable assessment of localized hydrocarbon resources over the whole area. For this reason, it is inadvisable to use standard tools for assessing the economic efficiency of a project.

In the framework of this master's thesis, the capital expenditures for construction of the production platform being the main technical mean for the development, was estimated using the database of offshore oil and gas projects prepared by WoodMackenzie.

When estimating CAPEX, the costs of various operating companies were taken into account at each stage of the platform construction:

- pre-FEED;
- FEED;
- Detailed Engineering ;
- Procurement and Construction;
- Installation.

Operational costs were not included in the assessment, as they directly depend on the operating conditions of the platform and vary within fairly wide limits.

At the stage of design and survey work, the following is taken into account in the structure of costs:

- design work;
- adjustment of the technical design and working design documentation;
- technical support of construction;
- labor costs.

During construction, the following costs are analyzed:

- construction at the shipyard;
- accompanying design;
- insurance of the object in the construction;
- material costs (purchases and services), namely the cost of materials, purchased components and equipment required for construction;
- labor costs.

To estimate capital expenditures, the world experience in construction of various platforms was used. Three criteria were used to distinguish the projects close to the concept proposed in this research:

- Platform type – gravity;

- Construction material – concrete or steel/concrete;
- Region – Arctic or sub-Arctic.

Table 38: Parameters of the selected platforms

Platform Name	Region	Type	Construction Material	Water Depth	Weight, tons	
					Foundation	Topside
Orlan	Sakhalin	Gravity	steel/concrete	16	30 000	10 000
Berkut	Sakhalin		concrete	35	156 400	42 780
Piltun-Astokhskaya B	Sakhalin		concrete	31	90 000	33 000
LUN-A	Sakhalin		concrete	48	103 000	27 400
Hibernia	Grand Banks		concrete	78	550 000	39 000
Hebron	Grand Banks		concrete	93	300 000	42 000
White Rose (Extension Project)	Grand Banks		concrete	123	210 000	30 000

According to water depth (height of the foundation), all these projects are close to the conditions of the North Wrangel license area.

Using the WoodMackenzie database, the costs were estimated at each stage of the platform construction. Additionally, the total costs were calculated and the platforms were ranked from less expensive to the most expensive. It should be noted that all values of capital expenditures were indexed (the beginning of 2018).

Table 39: CAPEX for the construction of various platforms, mln. USD

Platform Name	Pre-FEED	FEED	Detailed Engineering	Procurement and Construction	Installation	Total costs
Orlan	2,8	8,4	16,9	151,8	23	203
White Rose	6	18,2	36,7	340,7	53,4	455
Piltun-Astokhskaya B	7,4	22,2	44,5	400,2	60,6	535
LUN-A	12,4	37,3	74,6	671,4	101,7	897,4
Hibernia	13,2	39,6	79,2	713	108	953,1
Berkut	22,8	68,4	136,8	1 231,6	186,6	1 646,2
Hebron	47,5	142,6	285,1	2 381,0	356,4	3 212,7

Undoubtedly, it is impossible to draw a direct parallel between the cost of building the conceptually described production platform for the license area and the above mentioned platforms. Each project is unique. Countries constructing the platforms have different taxation systems, legislative frameworks governing this business, etc. The distances to which a platform should be transported, the costs of renting towing boats are also different, etc. However, the analysis is useful from the point of view of obtaining an understanding of the possible CAPEX levels.

Discussions and conclusion

Environmental conditions of the North Wrangel license area, main limiting factors, status of the Arctic field development technology, the most feasible technical solutions, recommended concepts of field development and oil transportation, ice and wave actions on the structures as well as CAPEX estimates were studied in the master's thesis.

The conducted studies within the master's thesis allowed:

- to reveal the range of existing technical and technological solutions applicable for the development of the East Siberian Sea hydrocarbon resources;
- to develop and test a new approach to the conceptual study held in lack-of-data conditions and based on a comparative analysis of environmental conditions of similar regions;
- to prepare an information basis that, with the required amount of field data, can be used to narrow further detailed conceptual analysis;
- to preliminarily assess the field development efficiency with emphasis on technological and economic aspects.

Feasibility of field development in the North Wrangel license area have been proven. According to preliminary estimates, the North Wrangel license area has a significant resource base. Characterized by particularly complex environmental conditions, it can also be perceived as a polygon for development of innovative technologies and consolidation of competencies. For instance, drilling rigs used today do not allow to complete exploratory drilling during one season in the East Siberian Sea. In this connection, it is necessary to design and build mobile ice-resistant drilling rigs capable of providing year-round drilling, and therefore, earlier commissioning of a field due to acceleration of a geological exploration program. Pre-project work in this field is already underway. Another promising direction is the transfer of these drilling rigs to production platforms, which will reduce the field development time and optimize the cash flow.

The implementation of these and other technological growth drivers combined with the use of well-proven technologies are important for strategic development and technical progress.

List of references

1. Gazprom Neft PJSC webpage. *The Reference Information published on Press Center tab* (in Russian).
Direct link (valid on 07.06.2018):
<http://www.gazprom-neft.ru/press-center/news/1108583/>
2. Gazprom Neft Sakhalin LLC webpage. *The company's projects description* (in Russian).
Direct link (valid on 07.06.2018):
<http://www.sakhalin.gazprom-neft.ru/business/about/>
3. Macnab, R., & Edwards, M. (2002, October) *Bathymetric Mapping of the North Polar Seas*. Report at a Workshop at the Hawaii Mapping Research Group, University of Hawaii, Honolulu, USA.
Direct link (valid on 07.06.2018):
<https://pdfs.semanticscholar.org/ce48/a9a0edcb2df7149398bf876a8c7e38a90095.pdf>
4. Arctic and Antarctic Research Institute webpage. *Arctic Ocean meteorological data*.
Direct link (valid on 07.06.2018):
<http://wdc.aari.ru/datasets/>
5. The webpage of the unified state information system on the situation in the world ocean (in Russian).
Direct link (valid on 07.06.2018):
<http://portal.esimo.ru/portal>
6. Sea Surface Salinity Remote Sensing at CATDS Ocean Salinity Expert Center (CEC-OS). *Salinity distribution in the Arctic Seas*.
Direct link (valid on 07.06.2018):
<http://www.salinityremotesensing.ifremer.fr/home>
7. Arctic and Antarctic Research Institute webpage. *Arctic Ocean hydrologic data*.
Direct link (valid on 07.06.2018):
<http://wdc.aari.ru/datasets/>
8. Palmer, A., & Croasdale, K. (2013). *Arctic offshore engineering*. World Scientific Publishing, Singapore.
9. Arctic and Antarctic Research Institute webpage. *Arctic Ocean ice data*.
Direct link (valid on 07.06.2018):
http://www.aari.ru/resources/a0011_12/manual_op/infoice/iceformation/vsb.html

10. Det Norske Veritas (2010). *Environmental conditions and environmental loads*, DNV-RP-C205.
Direct link (valid on 07.06.2018):
<https://rules.dnvgl.com/docs/pdf/dnv/codes/docs/2010-10/rp-c205.pdf>
11. *Proceedings of the 18th International Ship and Offshore Structures Congress* (ISSC 2012), Rostock, Germany.
Direct link (valid on 07.06.2018):
<http://www.issc2015.org/images/issc2012/issc2012-vol2.pdf>
12. Abramov, V. A. (1996). *Atlas of Arctic Icebergs: The Greenland, Barents, Kara, Laptev, East-Siberian and Chukchi Seas and the Arctic Basin*. Backbone Publishing Company.
13. Fadeev, A. (2015). *Current status of the Russian Arctic projects implementation by Gazprom Neft PJSC*, Gazprom Neft Sakhalin LLC.
14. MacCamy, R. C., & Fuchs, R. A. (1954). *Wave forces on piles: a diffraction theory* (No. TM-69). Corps of Engineers Washington DC Beach Erosion Board.
Direct link (valid on 07.06.2018):
http://acwc.sdp.sirsi.net/client/en_US/default/index.assetbox.assetactionicon.view/1007800?rm=TECHNICAL+MEMO2%7C%7C%7C1%7C%7C%7C0%7C%7C%7Ctrue
15. Gudmestad, O. (2015). *Marine Technology and Operations: Theory & Practice*. WIT Press.
16. International Organization for Standardization (2010). *Petroleum and natural gas industries – Arctic offshore structures*, ISO/FDIS 19906:2010(E).
Direct link (valid on 07.06.2018):
https://www.rosneft.com/upload/site2/01/ISO_19906.pdf
17. Løset, S., Shkhinek, K. N., Gudmestad, O. T., & Høyland, K. V. (2006). *Actions from ice on arctic offshore and coastal structures*. LAN.
18. Kadry, S. (2015). *Monte Carlo Simulation Using Excel: Case Study in Financial Forecasting*. In *The Palgrave Handbook of Research Design in Business and Management* (pp. 263-289). Palgrave Macmillan US.
Direct link (valid on 07.06.2018): https://link.springer.com/content/pdf/10.1007/978-1-137-48495-6_16.pdf
19. Belliveau, D. J., Hayden, H., & Prinsenber, S. (2002, January). *Ice Conditions at the Confederation Bridge-Winter 2000*. In *The Twelfth International*

- Offshore and Polar Engineering Conference. International Society of Offshore and Polar Engineers.
Direct link (valid on 07.06.2018):
http://www.bio.gc.ca/science/research-recherche/ocean/ice-glance/documents/Belliveau_1115p748.pdf
20. Sayeed, T., Colbourne, B., Quinton, B., Molyneux, D., Peng, H., & Spencer, D. (2017). *A review of iceberg and bergy bit hydrodynamic interaction with offshore structures*. Cold Regions Science and Technology, 135, 34-50.
Direct link (valid on 07.06.2018):
<http://www.sciencedirect.com/science/article/pii/S0165232X16303901#>
21. Ertle, R. E. (1974). *Statistical analysis of observed iceberg drift*. Arctic, 121-127.
Direct link (valid on 07.06.2018):
<http://pubs.aina.ucalgary.ca/arctic/Arctic27-2-121.pdf>
22. International Organization for Standardization (2016). *Petroleum and natural gas industries – Offshore production installations – Major accident hazard management during the design of new installations*, ISO 17776:2016.
Direct link (valid on 07.06.2018):
<https://www.iso.org/standard/63062.html>
23. Norwegian Technology Standards Institution (2001). *Risk and emergency preparedness analysis*, NORSOK Z-013 Rev. 2.
Direct link (valid on 07.06.2018):
<http://www.standard.no/pagefiles/955/z-013.pdf>
24. VNIIG named after B.E. Vendeev LLC (2012). *Loads and impacts on Hydraulic structures (from wave, ice and ships)*, SP 38.13330.2012 (in Russian).
Direct link (valid on 07.06.2018):
<http://docs.cntd.ru/document/1200095522>
25. Canadian Standards Association (2008). *General Requirements, Design Criteria, the Environment, and Loads*, CAN/CSA-S471-04 (R2008).
Direct link (valid on 07.06.2018):
<http://www.scc.ca/en/standardsdb/standards/19147>
26. Canadian Standards Association (2007). *Limit States Design of Steel Structures*, CAN/CSA-S16-01 (R2007).
Direct link (valid on 07.06.2018):
<https://www.scc.ca/en/standardsdb/standards/7696>

27. Wilson, J. F. (Ed.). (2003). *Dynamics of offshore structures*. John Wiley & Sons.
Direct link (valid on 07.06.2018):
<https://www.slideshare.net/HungNguyenManh/download-here-15062220>
28. Aurora, R. P., Ramsey, T. E., Shafer, R. S., Noble, P. G., Westerman, T. H., & Berta, D. P. (2014). U.S. Patent No. 8,821,071. *Conical piled monopod*. Washington, DC: U.S. Patent and Trademark Office.
Direct link (valid on 07.06.2018):
<https://www.google.com/patents/US20120128433>
29. About Planet webpage. *Picture of iceberg in the East Siberian Sea*.
Direct link (valid on 07.06.2018):
<https://about-planet.ru/priroda-azii/vostochno-sibirskoe-more>
30. Wikimapia webpage. *Bennett Island glacier cap*.
Direct link (valid on 07.06.2018):
<http://wikimapia.org/8341379/ru/%D0%9E%D1%81%D1%82%D1%80%D0%BE%D0%B2-%D0%91%D0%B5%D0%BD%D0%BD%D0%B5%D1%82%D1%82%D0%B0>
31. Gazprom Neft Shelf LLC (2011). *The company's feasibility report on IRGBS "Prirazlomnaya"* (in Russian).
Direct link (valid on 07.06.2018):
http://www.greenpeace.org/russia/Global/russia/report/Arctic-oil/Prirazlomnaya_environ_impact_assessment.pdf
32. Gazprom Neft Shelf LLC (2013). *The company's presentation materials on Prirazlomnoye field development* (in Russian).
Direct link (valid on 07.06.2018):
<http://docplayer.ru/38998721-Razrabotka-mestorozhdeniya-prirazlomnoe.html>
33. Neftegaz.RU webpage. *The technical library. Oil and Gas Fields* (in Russian).
Direct link (valid on 07.06.2018):
https://neftegaz.ru/tech_library/view/4070-Arkutun-Dagi
34. Zolotukhin, A.B., Gudmestad, O. T., Ermakov, A.I., Jakobsen, R.A., Mischenko, I.T., Vovk, V.S., Løset, S., Shkhinek, K. N. (2000). *Basics of the offshore oil and gas field development and construction of marine facilities in the Arctic*. "Oil and Gas" Publishers.
35. Exxon Neftegas Limited (2016). *Sakhalin-1 brochure 2016*. Exxon Neftegas Limited.
Direct link (valid on 07.06.2018):
http://cdn.sakhalin-1.com/~media/sakhalin/files/publications/sakhalin1_overview_brochure_2016.pdf

36. Exxon Neftegas Limited (2014). *Arkutun-Dagi, Berkut platform brochure 2014*. Exxon Neftegas Limited.
Direct link (valid on 07.06.2018):
http://cdn.sakhalin-1.com/~media/sakhalin/files/publications/berkut_2014.pdf
37. Husky Oil Operations Ltd. (2001). *White Rose Oilfield Development Application. Volume 2 Development Plan*. St. John, NL. Husky Energy.
Direct link (valid on 07.06.2018):
http://www.huskyenergy.ca/downloads/areasofoperations/eastcoast/DevelopmentApplication/Vol_2_Introduction.pdf
38. Hibernia webpage. *The project's main page*.
Direct link (valid on 07.06.2018):
<http://www.hibernia.ca/>
39. Canada – Newfoundland & Labrador Offshore Petroleum Board webpage. *Production Data tab*.
Direct link (valid on 07.06.2018):
<http://www.cnlopb.ca/information/statistics.php#rm>
40. Offshore Technology journal webpage. *Hibernia Oil and Gas Field Project*.
Direct link (valid on 07.06.2018):
<https://www.offshore-technology.com/projects/hibernia/>
41. Hebron Project webpage. *The project description tab*.
Direct link (valid on 07.06.2018):
<http://www.hebronproject.com/project/index.aspx>
42. Hebron Project (2012). *Hebron Project Expression of Interest. Offshore Loading System*. Hebron.
Direct link (valid on 07.06.2018):
<http://www.hebronproject.com/docs/procurement/ols.pdf>
43. Husky Energy Ltd. (2012). *White Rose Extension Project. Project Description*. Husky Energy.
Direct link (valid on 07.06.2018):
http://wwrp.huskyenergy.com/Project_overview
44. Norman, P., Lochte, G., & Hurley, S. (2008). *White Rose: Overview of current development and plans for future growth*. Proceedings of the 18th International Offshore and Polar Engineering Conference, Vancouver, Canada. International Society of Offshore and Polar Engineers.
Direct link (valid on 07.06.2018):
https://www.onepetro.org/conference-paper/ISOPE-I-08-267?sort=&start=0&q=White+Rose%3A+Overview+of+Current+Development+and+Plans+for+Future+Growth&from_year=&peer_reviewed=&published_between=&fromSearchResults=true&to_year=&rows=10#

45. Van Es, B., Pille, N., de Vlaming, R., and de Vries, J. (2004). *Construction of wellhead protection glory holes for White Rose Project, Canada*. Terra et Aqua.
Direct link (valid on 07.06.2018): https://www.researchgate.net/publication/297841099_Construction_of_wellhead_protection_Glory_Holes_for_White_Rose_Project_Canada
46. Popp, B. (2006). *The First Alaskan Oil & Gas Experience. The Cook Inlet Basin*. Presentation.
Direct link (valid on 07.06.2018): http://www.empr.gov.bc.ca/Mining/Geoscience/MapPlace/thematicmaps/OffshoreMapGallery/Documents/BillPoppSep21_04.pdf
47. The United States Geological Survey. *National Oil and Gas Assessment Tab*.
Direct link (valid on 07.06.2018): <https://energy.usgs.gov/OilGas/AssessmentsData/NationalOilGasAssessment/USBasinSummaries.aspx?provcode=5003>
48. Belmar Engineering Services Ltd. (2009). *Platform Information, Cook Inlet, Alaska*. Cook Inlet Regional Citizens Advisory Council.
Direct link (valid on 07.06.2018): <https://www.circac.org/wp-content/uploads/Platform-Information-Cook-Inletpdf.pdf>
49. Timco, G.W. and Frederking, R. (2009). *Overview of Historical Canadian Beaufort Sea Information*. Technical Report. NRC Canadian Hydraulics Centre.
Direct link (valid on 07.06.2018): <https://www.restco.ca/NRC%20CHC%20Beaufort%20Sea%20History%20Feb%202009%20%2099%20pp.pdf>
50. Zolotukhin, A.B. (2016). *Offshore Field Development with emphasis on the Arctic*. Lecture Course. Gubkin University.
51. Zolotukhin, A., & Gavrilov, V. (2011). *Russian Arctic petroleum resources: challenges and future opportunities*. OTC Arctic Technology Conference. Offshore Technology Conference.
Direct link (valid on 07.06.2018): <https://www.restco.ca/NRC%20CHC%20Beaufort%20Sea%20History%20Feb%202009%20%2099%20pp.pdf>
52. Prokhorov, A. M. (1974). *Great Soviet Encyclopedia* (in Russian).
53. Gazprom Neft Shelf LLC (2018). *Geological information was obtained in oral conversations with the company's specialists*.
54. Pevek City District (2018). *Official information and statistics of the city of Pevek* (in Russian)
Direct link (valid on 07.06.2018): <https://go-pevek.ru>

55. Federal Agency of Sea and River Transport (2018). *Information tab about the Northern Sea Route* (in Russian)
Direct link (valid on 07.06.2018): http://www.morflot.ru/deyatelnost/morskoy_flot/ledokolnoe_obespechenie_/severnoyiy_morskoy_put.html
56. Pivivarov, K.N., Zolotukhin, A.B. (2017). *Review of methods for clustering and ranking of technological accessibility of the Arctic seas by the example of the Barents Sea* (in Russian). Oil Industry Journal.
Direct link (valid on 07.06.2018): http://www.oil-industry.net/Journal/archive_detail.php?ID=11117&art=230565
57. Orlov, A.I. (2009). *About the development of mathematical methods of classification theory* (in Russian). Diagnostics of materials.
58. Kendall, M., Stewart, A. (1976). *Multivariate statistical analysis and time series* (in Russian). The Science.
59. Lisenkov, A.N., Yarkovskaya, T.V. (2009). *Expert evaluation in management tasks*. Moscow State Transport University.
Direct link (valid on 07.06.2018): <http://library.miit.ru/methodics/10-1540.pdf>
60. DeGeer, D., Pauline, M., Lenan, G., Brand, J. (2012). *Survey of Arctic & Cold Regions Technology for Offshore Field Development*. Offshore Magazine, INTECSEA Inc.
61. Vyakhirev, R.I., Nikitin, B.A., Mirzoyev, D.A. (1999). *Arrangement and Development of the Oil and Gas Offshore Fields* (in Russian). Academy of Mining Sciences Publishing House.
62. National Petroleum Council, NPC (2015). *Arctic Subsea Pipelines and Subsea Production Facilities*. Technology & Operations Subgroup (paper #6-6).
Direct link (valid on 07.06.2018): http://www.npcarcticpotentialreport.org/pdf/tp/6-6_Arctic_Subsea_Pipelines_and_Subsea_Production_Facilities.pdf
63. Hannus, H. (2013). *Arctic Drillship*. Aker Solutions. NTNU.
64. WoodMackenzie (2018). *Database of offshore oil and gas projects*.
Direct link (valid on 07.06.2018): <https://www.woodmac.com/>
65. Ermakov, A.I. (2017). *Design methodology in the oil and gas industry and project management*. Lecture Course. Gubkin University.

Appendix A

A-1 Matlab code for ice loads on vertical structure simulation

```
clear all;
close all;
D=100;
m=0.9;
x=0:0.01:10;

pd_sigmaC=makedist('Normal','mu', 3.13, 'sigma',0.67);
pd_ice=makedist('Normal','mu', 1.55, 'sigma',0.283);
pd_I=makedist('Normal','mu', 3.75, 'sigma',0.25);
pd_K=makedist('Normal','mu', 0.075, 'sigma',0.0183);
iterations=1000;
hFig = figure('units','normalized','outerposition',[0 0 1 1]);

for i=1:iterations
    h(i,1)=random(pd_ice);
    sigmaC(i,1)=random(pd_sigmaC);
    I(i,1)=random(pd_I);
    K(i,1)=random(pd_K);
    F(i,1)=I(i)*K(i)*m*sigmaC(i)*D*h(i);
    pdf_ice=pdf(pd_ice,x);
    cdf_ice=cdf(pd_ice,x);
    pdf_sigmaC=pdf(pd_sigmaC,x);
    cdf_sigmaC=cdf(pd_sigmaC,x);
    pdf_I=pdf(pd_I,x);
    cdf_I=cdf(pd_I,x);
    pdf_K=pdf(pd_K,x);
    cdf_K=cdf(pd_K,x);

    if i>5
        subplot(2,2,1);
        histfit(F);
        xlabel('F, MN');
        ylabel('number of appearance, [1]');
        axis([0 400 0 inf]);

        subplot(2,2,2);
        f=0:0.01:400;
        pd_F=fitdist(F,'Normal');
        pdf_F=pdf(pd_F,f);
        cdf_F=cdf(pd_F,f);
        plot(i,pd_F.sigma/pd_F.mu*100,'.r'); hold on;
        grid on;
        axis([0 iterations 0 inf] )
        xlabel('iteration number');
        ylabel('\sigma / \mu, %');

        subplot(2,2,3);
        plot(f, cdf_F);
        xlabel('F, MN');
```

```

ylabel('CDF(F), [1]');
grid on;

subplot(2,2,4);
if i>6
    set(h1,'Visible','off');
    set(h2,'Visible','off');
    set(h3,'Visible','off');
    set(h4,'Visible','off');
    set(h5,'Visible','off');
    set(h6,'Visible','off');
    set(h7,'Visible','off');
end
edf_F=1-cdf_F;
h1=plot(f, edf_F);hold on;
set(gca, 'YScale', 'log');
axis([0 400 10^-5 1]);
xlabel('F, MN');
ylabel('EDF(F), [1]');
grid on;

SL=max(find(edf_F>10^-1));
a=SL;
h2=stem(f(a),edf_F(a),'.g');
xx=[0 f(a)]; yy=[edf_F(a) edf_F(a)];
h3=plot(xx,yy,'g');

ELIE=max(find(edf_F>10^-2));
a=ELIE;
h4=stem(f(a),edf_F(a),'.r');
xx=[0 f(a)]; yy=[edf_F(a) edf_F(a)];
h5=plot(xx,yy,'r');

ALIE=max(find(edf_F>10^-4));
a=ALIE;
h6=stem(f(a),edf_F(a),'.black');
xx=[0 f(a)]; yy=[edf_F(a) edf_F(a)];
h7=plot(xx,yy,'black');

pause(0.001);
end
end

```


A-2 Matlab code for ice loads on sloping structure simulation

```
clear all;
close all;
D=100;
RoW=1023;
RoI=884;
E=8700000000;
g=9.81;
C1=2.01;
C2=1.65;
x=0:0.01:2.5;

pd_Z=makedist('Normal','mu', 9.679, 'sigma',1.210);
pd_sigmaF=makedist('Normal','mu', 450000, 'sigma',90000);
pd_ice=makedist('Normal','mu', 1.55, 'sigma',0.283);
iterations=1000;
hFig=figure('units','normalized','outerposition',[0 0 1 1]);

for i=1:iterations
    Z(i,1)=random(pd_Z);
    sigmaF(i,1)=random(pd_sigmaF);
    h(i,1)=random(pd_ice);

    F(i,1)=(D*(sigmaF(i)*((RoW*g*((h(i))^5)/E)^0.25)*C1+(Z(i)*h(i)*RoI*g*C2))/(1
    0^6);
    pdf_Z=pdf(pd_Z,x);
    cdf_Z=cdf(pd_Z,x);
    pdf_sigmaF=pdf(pd_sigmaF,x);
    cdf_sigmaF=cdf(pd_sigmaF,x);
    pdf_ice=pdf(pd_ice,x);
    cdf_ice=cdf(pd_ice,x);

    if i>5
        subplot(2,2,1);
        histfit(F);
        xlabel('F, MN');
        ylabel('number of appearance, [1]');
        axis([0 60 0 inf]);

        subplot(2,2,2);
        f=0:0.01:60;
        pd_F=fitdist(F,'Normal');
        pdf_F=pdf(pd_F,f);
        cdf_F=cdf(pd_F,f);
        plot(i,pd_F.sigma/pd_F.mu*100,'.r'); hold on;
        grid on;
        axis([0 iterations 0 inf] )
        xlabel('iteration number');
        ylabel('\sigma / \mu, %');

        subplot(2,2,3);
        plot(f, cdf_F);
        xlabel('F, MN');
```

```

ylabel('CDF(F), [1]');
grid on;

subplot(2,2,4);
if i>6
    set(h1,'Visible','off');
    set(h2,'Visible','off');
    set(h3,'Visible','off');
    set(h4,'Visible','off');
    set(h5,'Visible','off');
    set(h6,'Visible','off');
    set(h7,'Visible','off');
end
edf_F=1-cdf_F;
h1=plot(f, edf_F);hold on;
set(gca, 'YScale', 'log');
axis([0 60 10^-5 1]);
xlabel('F, MN');
ylabel('EDF(F), [1]');
grid on;

SL=max(find(edf_F>10^-1));
a=SL;
h2=stem(f(a),edf_F(a),'.g');
xx=[0 f(a)]; yy=[edf_F(a) edf_F(a)];
h3=plot(xx,yy,'g');

ELIE=max(find(edf_F>10^-2));
a=ELIE;
h4=stem(f(a),edf_F(a),'.r');
xx=[0 f(a)]; yy=[edf_F(a) edf_F(a)];
h5=plot(xx,yy,'r');

ALIE=max(find(edf_F>10^-4));
a=ALIE;
h6=stem(f(a),edf_F(a),'.black');
xx=[0 f(a)]; yy=[edf_F(a) edf_F(a)];
h7=plot(xx,yy,'black');

pause(0.001);
end
end

```

A-3 Matlab code for iceberg load simulation

```
clear all;
close all;
H=5;
Ro=884;
Cm=0.2;
Z=0.001;
x=0:0.01:10;

pd_V=makedist('Normal','mu', 0.179, 'sigma',0.002);
pd_L=makedist('Normal','mu', 85, 'sigma',21.67);
pd_B=makedist('Normal','mu', 47.5, 'sigma',12.5);
iterations=1000;
hFig = figure('units','normalized','outerposition',[0 0 1 1]);

for i=1:iterations
    L(i,1)=random(pd_L);
    V(i,1)=random(pd_V);
    B(i,1)=random(pd_B);
    F(i,1)=((1/Z)*0.5*H*L(i)*B(i)*Ro*(1+Cm)*(V(i))^2)/1000000;
    pdf_L=pdf(pd_L,x);
    cdf_L=cdf(pd_L,x);
    pdf_B=pdf(pd_B,x);
    cdf_B=cdf(pd_B,x);
    pdf_V=pdf(pd_V,x);
    cdf_V=cdf(pd_V,x);

    if i>5
        subplot(2,2,1);
        histfit(F);
        xlabel('F, MN');
        ylabel('number of appearance, [1]');
        axis([0 1000 0 inf]);

        subplot(2,2,2);
        f=0:0.01:1000;
        pd_F=fitdist(F,'Normal');
        pdf_F=pdf(pd_F,f);
        cdf_F=cdf(pd_F,f);
        plot(i,pd_F.sigma/pd_F.mu*100,'.r'); hold on;
        grid on;
        axis([0 iterations 0 inf] )
        xlabel('iteration number');
        ylabel('\sigma / \mu, %');

        subplot(2,2,3);
        plot(f, cdf_F);
        xlabel('F, MN');
        ylabel('CDF(F), [1]');
        grid on;

        subplot(2,2,4);
        if i>6
            set(h1,'Visible','off');
            set(h2,'Visible','off');
            set(h3,'Visible','off');
            set(h4,'Visible','off');
```

```

        set(h5, 'Visible', 'off');
        set(h6, 'Visible', 'off');
        set(h7, 'Visible', 'off');
    end
    edf_F=1-cdf_F;
    h1=plot(f, edf_F);hold on;
    set(gca, 'YScale', 'log');
    axis([0 1000 10^-5 1]);
    xlabel('F, MN');
    ylabel('EDF(F), [1]');
    grid on;

    SL=max(find(edf_F>10^-1));
    a=SL;
    h2=stem(f(a), edf_F(a), '.g');
    xx=[0 f(a)]; yy=[edf_F(a) edf_F(a)];
    h3=plot(xx, yy, 'g');

    ELIE=max(find(edf_F>10^-2));
    a=ELIE;
    h4=stem(f(a), edf_F(a), '.r');
    xx=[0 f(a)]; yy=[edf_F(a) edf_F(a)];
    h5=plot(xx, yy, 'r');

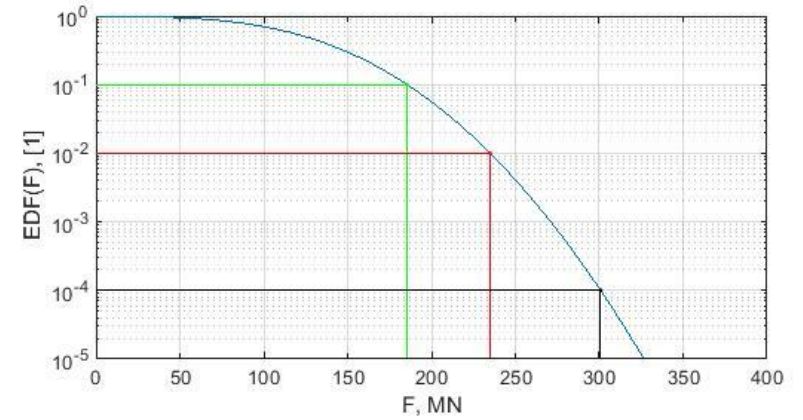
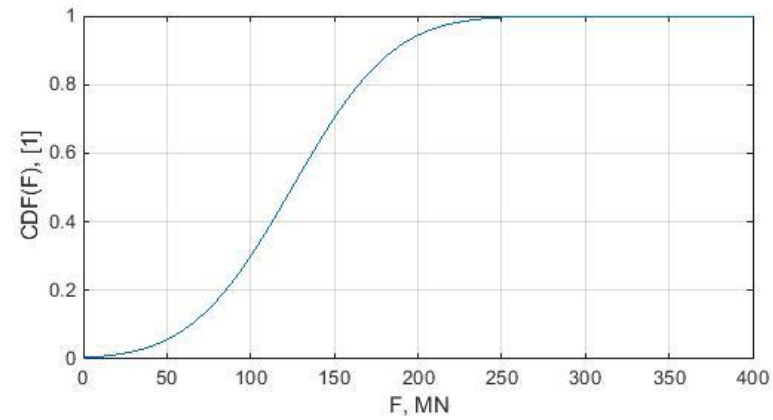
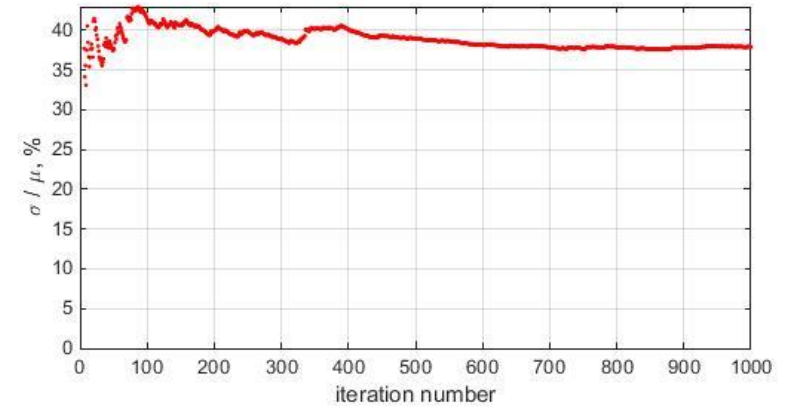
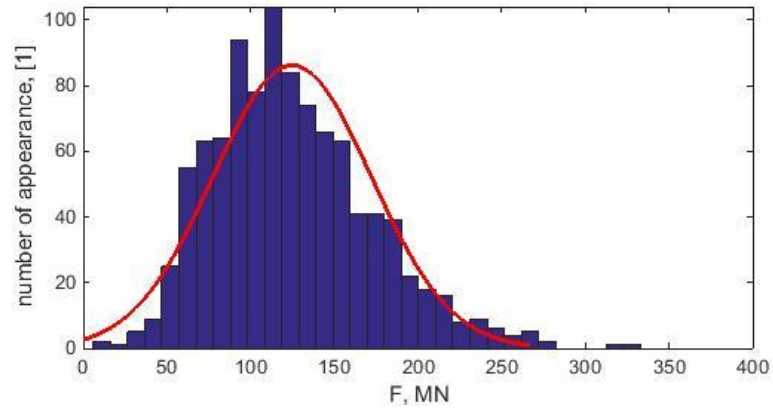
    ALIE=max(find(edf_F>10^-4));
    a=ALIE;
    h6=stem(f(a), edf_F(a), '.black');
    xx=[0 f(a)]; yy=[edf_F(a) edf_F(a)];
    h7=plot(xx, yy, 'black');

    pause(0.001);
end
end

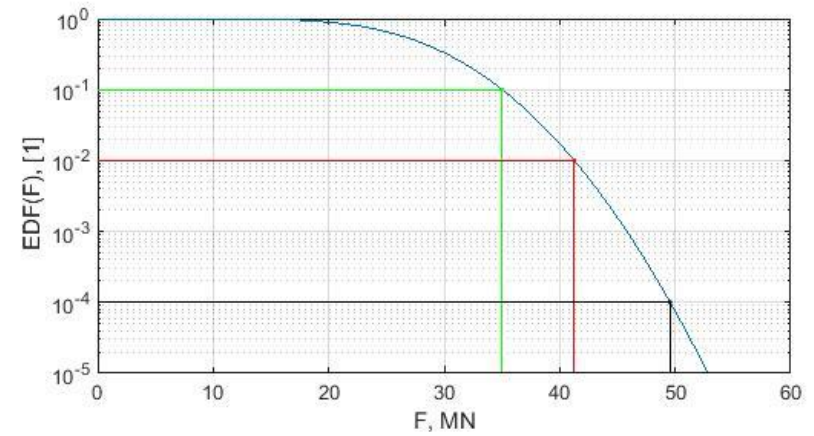
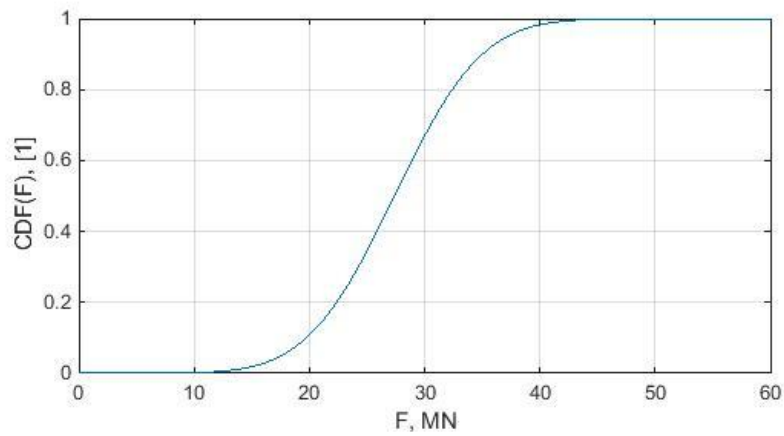
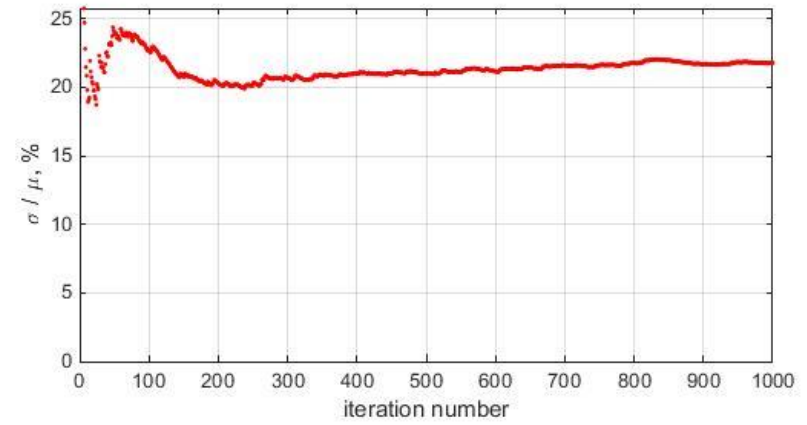
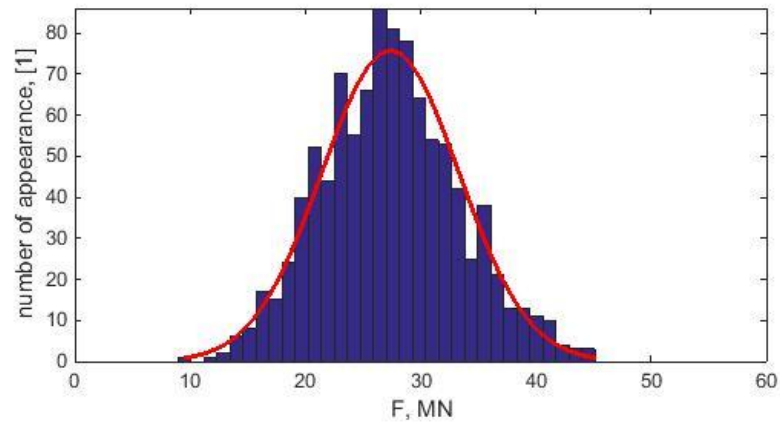
```

Appendix B

B-1 The simulation results (for vertical walls)



B-2 The simulation results (for sloping walls)



B-3 The simulation results (iceberg impact)

